HOBE

The Danish Hydrological Observatory

Jensen, Karsten H.; Refsgaard, Jens Christian

Published in:
Vadose Zone Journal

DOI:
10.2136/vzj2018.03.0059

Publication date:
2018

Document version
Publisher's PDF, also known as Version of record

Published November 8, 2018

Special Section: Hydrological Observatories

Core Ideas

- HOBE provides an experimental catchment infrastructure.
- Measurements, experiments, and modeling are carried out.
- A number of research questions are addressed; the primary one is closure of the water balance.
- The database is available for data sharing.

HOBE: The Danish Hydrological Observatory

Karsten H. Jensen* and Jens Christian Refsgaard

The Danish hydrological observatory was established in 2007 in a catchment in the western part of Denmark representing hydrological conditions in a temperate climate with groundwater-dominated streamflow. In the catchment, an experimental infrastructure has been established where measurements, experiments, and modeling are performed across a range of spatial and temporal scales. The primary research question is water balance closure at different scales, which has been addressed using improved measurement and modeling methods. In addition, an array of research questions are related to processes in the individual hydrological compartments as well as the interactions between them. We provide here an overview of long-term monitoring and observation, dedicated observations, experiments, and modeling. An overview of main research findings is also provided. The research has provided new insights into the dynamics of the individual hydrological processes and their interactions. The hydrological fluxes are now determined with greater certainty, and the water balance is better constrained at different spatial scales.

Abbreviations: AEM, airborne electromagnetic; DMI, Danish Meteorological Institute; DTS, distributed temperature sensing; EOF, empirical orthogonal functions; ERT, electrical resistivity tomography; ET, evapotranspiration; RCM, regional-scale climate model; RMSE, root mean square error; SMAP, Soil Moisture Active Passive mission; SMOS, Soil Moisture and Ocean Salinity; UAV, unmanned aerial vehicle.

Closure of the water balance has been a critical problem in Denmark when modeling the water circulation at catchment scale. When using independent measurements and assessments of hydrological fluxes, the water balance cannot be closed. This problem has propagated into assessments of the available water resources for water supply, which thus are inherently uncertain (Henriksen et al., 2003).

Water management assessments and decisions must be performed at catchment scale according to the European Water Framework Directive. This is a logical development because it is at larger scales that the hydrological and economic impacts due to climate change and human interferences can be managed. The closure problem as well as the insufficient knowledge of the hydrological fluxes at catchment scale imply that such assessments are taken on a highly uncertain basis. The hydrological uncertainty is related to several factors, including measurement and theoretical limitations. Basic hydrological fluxes, such as precipitation and evapotranspiration (ET), are difficult to measure reliably even at local scale, which translate into uncertainties of estimation of, for example, recharge. Other contributing factors to the water balance closure problem are measurement inaccuracies of stream flow and uncertainties regarding groundwater fluxes across catchment divides and deep groundwater flow to the sea.

However, the water balance closure problem at catchment scale is not only caused by measurement errors at the local scale. Regionalization of the measurements is also a contributing factor. At catchment scale, the number of measurement locations is sparse when considering traditional measurement techniques. This problem has been exacerbated in recent years as more and more traditional monitoring stations have been taken out of operation, leading to high levels of uncertainty when regionalizing the data to catchment-wide scale (He et al., 2013b). Thus, new innovative measurement and estimation techniques that go beyond traditional point measurements are needed (e.g., weather radar as well as airborne and satellite-borne sensors).

An improved knowledge of the states within the catchment as well as the internal fluxes is also needed to understand catchment behavior. Soil moisture is a critical variable

K.H. Jensen, Dep. of Geosciences and Natural Resource Management, Univ. of Copenhagen, Øster Voldgade 10, 1350-Copenhagen K., Denmark; J.C. Refsgaard, Geological Survey of Denmark and Greenland, Øster Voldgade 10, 1350-Copenhagen K., Denmark. *Corresponding author (khj@ign.ku.dk).

Received 31 Mar. 2018.
Accepted 15 July 2018.

Citation: Jensen, K.H., and J.C. Refsgaard. 2018. HOBE: The Danish hydrological observatory. Vadose Zone J. 17:180059. doi:10.2136/vzj2018.03.0059

in this regard because it controls the division of precipitation into ET, lateral runoff, and recharge. Commonly used sensors provide measurements with small spatial support, and the relevance of such measurements at larger scale can be questioned. Development of new measurement techniques at a more appropriate spatial scale is required to obtain relevant information of this variable, for example hydrogeophysical measurements (Binley et al., 2015) or the cosmic ray neutron technique (Andreasen et al., 2017a).

Improving the understanding of catchment scale behavior also requires that the internal fluxes between the hydrological compartments be better quantified. Important internal fluxes are groundwater–surface water interactions, recharge to the water table, and fluxes between aquifers. These fluxes may be estimated using tracers such as heat (Sebok et al., 2013) and stable isotopes (Müller et al., 2017) as well as traditional hydraulic head measurements in three-dimensional arrays.

Merging catchment-wide measurements and observations as well as new theoretical findings demands spatially distributed and integrated hydrological models that consider interactions between soil, vegetation, atmosphere, aquifer systems, streams, lakes, and the marine environment. Only these models are capable of making such integrations and make optimal use of all data and thereby provide a coherent description of catchment behavior as well as reliable predictions of the consequences of, for example, climate and land use change (Vereecken et al., 2015). Development and validation of such models and reliable quantification of the uncertainty in predictions require a solid database of spatial and temporal data. In this regard, hydrological observatories are crucial instruments.

As described in this special issue, several hydrological observatories have been established in recent years. The Danish Hydrological Observatory and Exploratorium (HOBE) was established in 2007 with the objective to create an experimental catchment infrastructure where measurements, experiments, and modeling are performed over a range of spatial and temporal scales to address an array of research questions contributing to the main research question, which is the closure of the water balance at different spatial scales. The observatory represents hydrological conditions in a temperate climate with groundwater-dominated streamflow. The catchment is as such complementary to other hydrological observatories described in this special issue.

We have specifically focused on the following goals in our research:

- Improvements of independent estimation of basic hydrological fluxes including precipitation, ET, recharge, groundwater–surface water interactions, and stream discharge.
- Improved quantitative precipitation estimation based on an improved bias correction model for rain gauge data as well as on weather radar data.
- Development and testing of models of energy fluxes over different land-surface types.
- Application of nature's own tracers, temperature, and stable isotopes for improving the estimation of groundwater–surface water interactions.
- Estimation of spatial and temporal variation of the state variable soil moisture across the catchment using data representing different temporal and spatial scales.
- Calibration/validation of remote sensing products.
- Development of integrated hydrological models and coupled climate–hydrological models.
- Improved calibration of integrated hydrological models using different types of data representing different spatial and temporal scales.
- Assimilation and integration of new data types (ground-, air-, and satellite-based hydrological and geophysical data) in integrated hydrological models.
- Development of spatial performance metrics for calibration and validation of distributed and integrated hydrological models.
- Analysis of uncertainty propagation in hydrological models.
- Water balance assessments at various scales, from the local field scale (<1 km^2), to sub-catchment scale (~100–1000 km^2), to catchment scale (~2500 km^2), and to the entire model area (~3500 km^2).

The HOBE hydrological observatory is located in the Skjern catchment in western Denmark. The observation, measurement, and modeling activities are performed in a nested approach where the following scales are considered (Fig. 1): (i) total Ringkøbing Fjord area (3500 km^2), (ii) Skjern catchment (2500 km^2), (iii) Ahlergaarde catchment (1050 km^2), (iv) Holtum catchment (106 km^2), and (v) Abild catchment (67 km^2).

In addition, local sites for detailed measurements and experimental activities have been established: (i) four local field observatories representing the land surfaces agriculture, forest, meadow grassland, and heathland; (ii) a local field observatory for stream–groundwater interaction; and (iii) a local field observatory for lagoon–groundwater interaction.

The HOBE hydrological observatory was established primarily by funding from the private VILLUM Foundation. The presently secured lifetime of the full observatory is throughout 2019. The three flux stations in the observatory are now part of the national ICOS infrastructure, and their operations are secured until 2021.

Catchment Characteristics

The Skjern catchment is located in western Denmark (Fig. 1). It is drained by the Skjern River and its tributaries and discharges into the Ringkøbing brackish lagoon toward west. The lagoon is connected to the North Sea through a sluice, which regulates the water exchange between the two water bodies. The Skjern River is the river in Denmark with the largest mean annual discharge, which is ~35 $m^3 s^{-1}$. The area of the entire catchment is 2500 km^2; however, the observatory is nested by several subcatchments, the most important one being the Ahlergaarde subcatchment (1050 km^2), where most of the measurement and modeling studies are performed. The second most important one is the Holtum

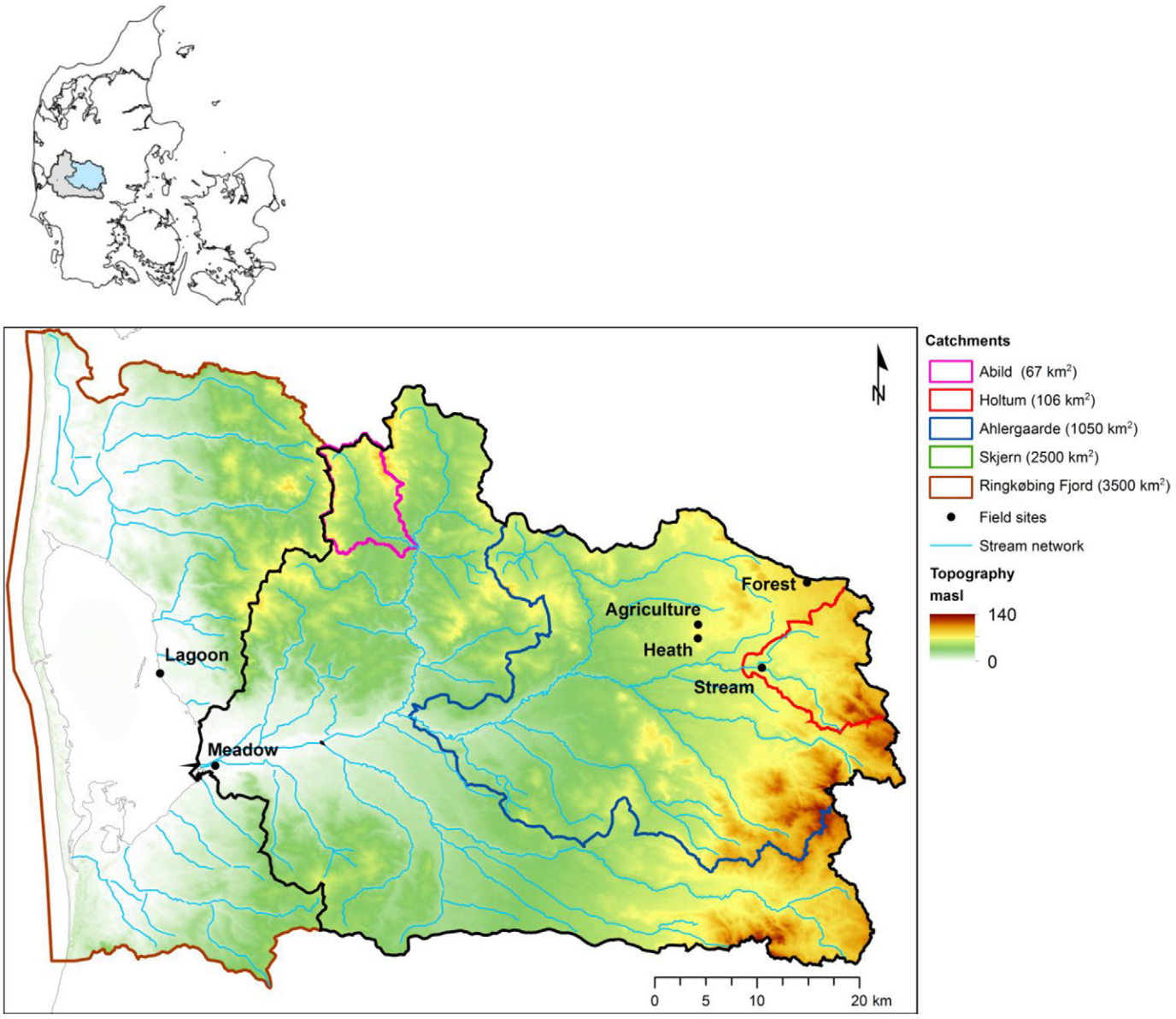

Fig. 1. Skjern catchment and subcatchments.

subcatchment (106 km^2), where groundwater–surface water interaction is studied extensively.

The topography is relatively flat. The surface elevations in the eastern part of the catchment are ~125 m above sea level at the Jutland ridge and gently decreasing to sea level elevations toward the coast. The topography is partly shaped by the latest glaciation period (Weichel) when the glacier front at the maximum advance was located along a north–south line through Jutland and partly by the previous glaciation period (Saale), from which remnants are present mainly in the northwest of the catchment (Houmark-Nielsen and Kjaer, 2003) (Fig. 2).

Alluvial outwash deposits in the form of sand and gravel dominate the central part of the catchment. Toward the east, glacial deposits of moraine till are present with a higher content of clay. Also, the remnants from the Saale glaciation have higher clay content, and the dominant sediment type at these locations is clayey sand. Overall, the top sediments are highly permeable with little water retention capability, and the stream flow is therefore dominated by groundwater inflow.

Based on a classification of the topsoil performed by Greve et al. (2007), four soil classes can be identified in the catchment (Stisen et al., 2011). By far the dominant soil type is fine/coarse sandy soil (Fu et al., 2011).

The Quaternary deposits have a thickness <50 m in the eastern and central part of the area. Thickness increases to 250 m toward the west (Scharling et al., 2009; Stisen et al., 2011). Sand dunes are also present in the area. The Quaternary deposits are underlain by Miocene sediments in the form of alternating layers of marine, lacustrine, and fluvial deposits forming layers of clay, silt, sand, and gravel. Further below, thick layers of Paleogene clay

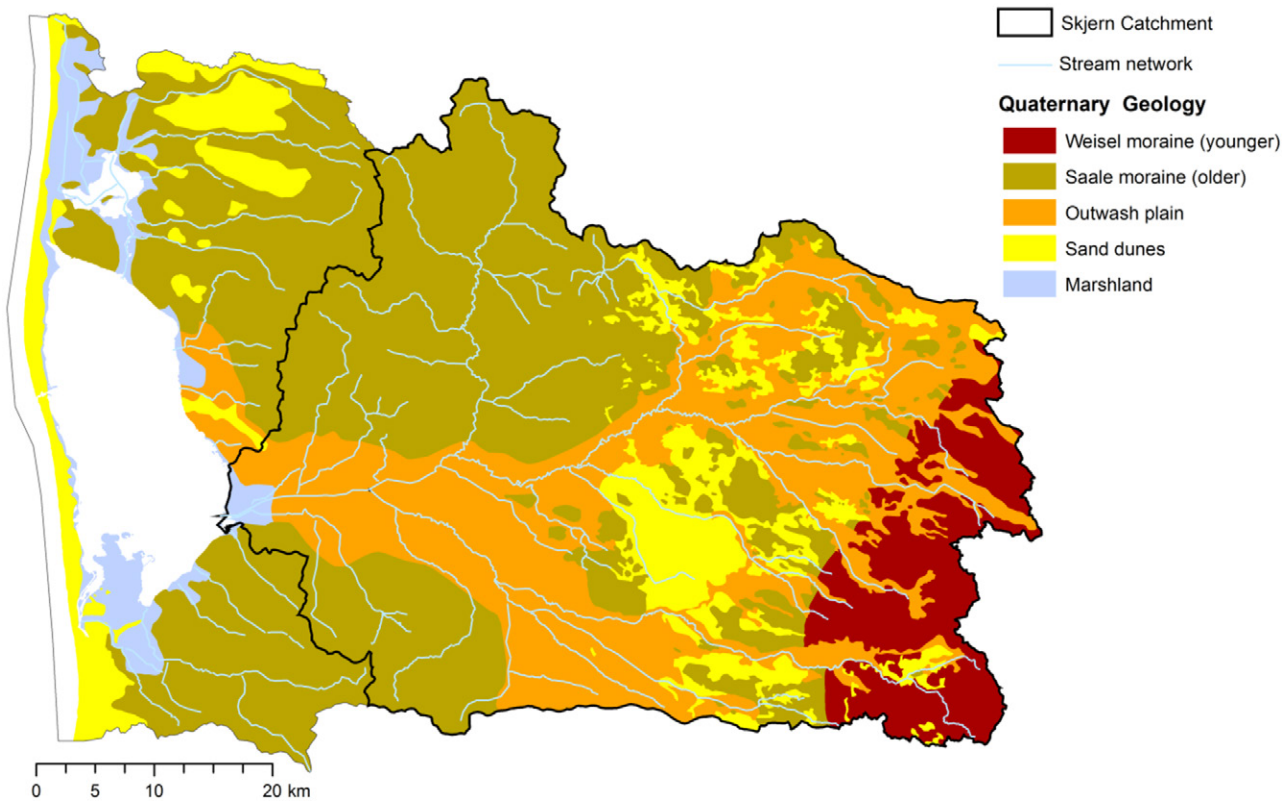

Fig. 2. Landscape elements (from Jensen and Illangasekare, 2011).

are found with little permeability and thus act as a lower impermeable boundary for the aquifer systems. The sand and gravel layers from the Quaternary and Miocene periods form interconnected aquifer systems (Stisen et al., 2011). A conceptualization of the geology is shown in Fig. 3 as a cross-section. The figure shows how the geological settings are conceptualized in most of the modeling studies performed within the framework of HOBE. The geological characterization is based on borehole descriptions, geophysical logs, and seismic data. Near the surface, a shallow layer (3 m) is located. Below, the Quaternary deposits are categorized into sand and clay, and the pre-Quaternary deposits are categorized as Miocene quartz sand, Miocene mica sand, and clay (He et al., 2013b). Each

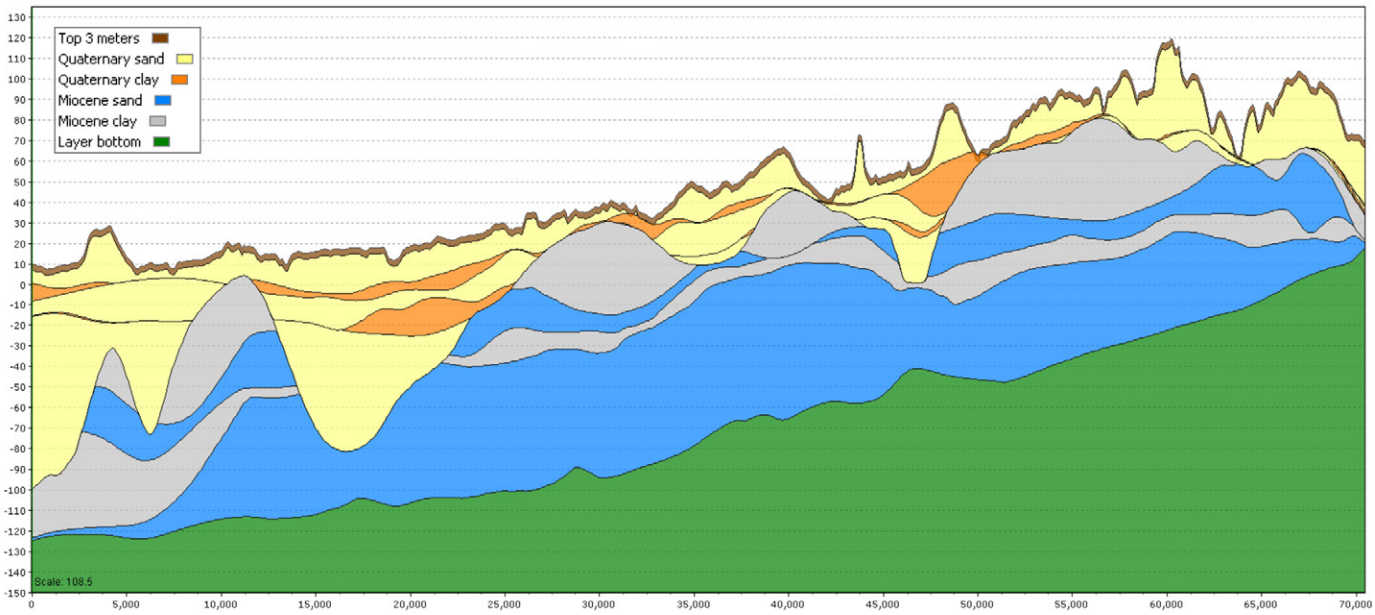

Fig. 3. Geological profile across the catchment in the west–east direction (reproduced from He et al., 2013b).

of these geological units is assigned uniform hydraulic parameters in the hydrological models.

The land surface of the catchment is predominantly agriculture, and, due to the sandy soil characteristics, extensive irrigation of the agricultural crops takes place. Based on satellite data, the land-use distribution is estimated as follows: grain and corn (55%), grass (30%), forest (7%), heath (5%), urban (2%), and other (1%) (Fig. 4) (Jensen and Illangasekare, 2011).

The climate of the observatory is of maritime origin and is influenced by weather systems coming from the Atlantic Ocean (van Roosmalen et al., 2007). The weather conditions are variable with frequent precipitation. The prevailing winds from the west lead to relatively mild winters and cool summers. The mean annual precipitation is about 1050 mm yr^{-1}, with the highest amounts in the months of October through December and lowest in the months of April and May. The mean annual temperature is 8.2°C. The highest mean monthly temperature is in August (16.5°C), and the lowest is in January (1.4°C). Precipitation in the form of snow is highly variable from year to year; in some years, no snowfall occurs, and in other years snow may stay on the ground for months.

Long-Term National Monitoring and Observations

Data Collection

Basic meteorological and hydrological variables (precipitation, climatic variables, stream discharge, and groundwater levels) have been measured for many decades as part of the national monitoring programs (Table 1).

To measure precipitation, the first gauges were installed in 1870 for manual reading of the daily precipitation catch. The network was gradually expanded and obtained the densest coverage toward the end of the last century. The Danish Meteorological Institute (DMI) is responsible for collecting, processing, and quality-checking of the data. For most years, the Hellmann rain gauge (Thedor Friedrichs Inc.) was the standard for manual reading. However, from about 2010, the density of the gauge network across Denmark, including the Skjern catchment, was significantly reduced when moving from manual to automatic recording of precipitation (He et al., 2013b). The new standard precipitation gauge in use is Pluvio2 (OTT Hydromet), which provides measurements of both liquid and solid precipitation data with 10-min resolution.

Both the old and new rain gauges are subject to undercatch due to wind turbulence around the orifice and wetting loss (Allerup and Madsen, 1980). The undercatch varies with precipitation intensity and type, shielding of the gauge, and wind speed. Typical correction values are 15% for rain and 30% for snow. To correct for the bias in precipitation measurements, mean monthly corrections factors developed from a historical 30-yr record have often been used (Allerup et al., 1998). Stisen et al. (2011) tested this method against a dynamic correction method developed by Allerup et al. (1997), which uses data for daily wind speed and temperature. The two sets of precipitation products were used as input to a hydrological model for the Ahlergaarde catchment, and much

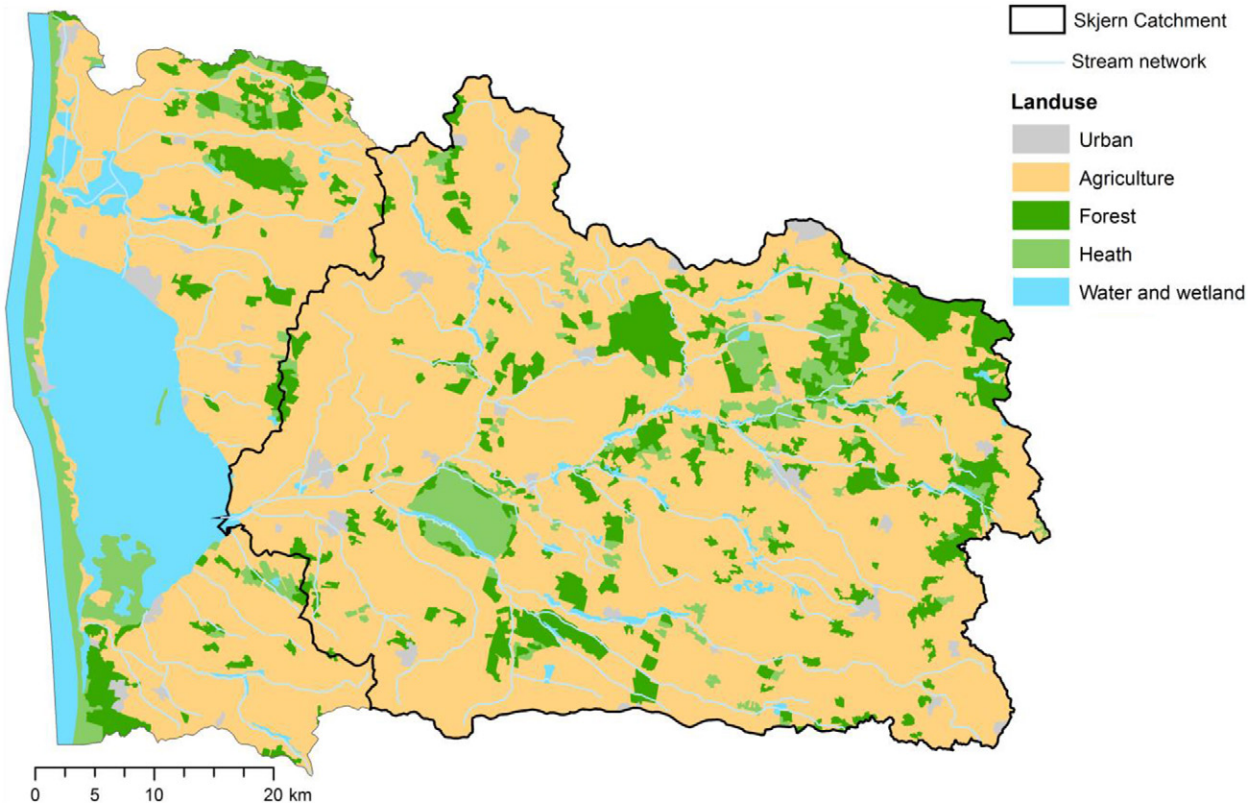

Fig. 4. Land surface classes (from Jensen and Illangasekare, 2011).

Table 1. National monitoring and observations within and in the neighborhood of the HOBE catchment.

Variable	No. of stations	Time period	Temporal resolution	Data provider
Precipitation				
Manual recording	33	1870–2009 (start times vary among the stations)	daily	Danish Meteorological Institute
Automatic recording	22	2010–present	10 min	Danish Meteorological Institute
Gridded precipitation product (10 by 10 km)		1989–present	daily	Danish Meteorological Institute
Climatic variables (incoming shortwave radiation, wind speed, relative humidity, air temperature, air pressure)	7	longest record from 1875	recent data hourly	Danish Meteorological Institute
Gridded climate data product (20 by 20 km)		1989–present	daily	Danish Meteorological Institute
Discharge	11	longest record from 1920	hourly	Danish Center for Environment and Energy
Observation wells	~3000	earliest observations from beginning of 1900	vary from well to well	Geological Survey of Denmark and Greenland

better model performance was obtained when using the dynamic correction method. This has become the standard method for precipitation correction in Denmark (Stisen et al., 2012).

Currently, 22 automatic recording precipitation stations are in operation in and adjacent to the Skjern catchment (Table 1). The locations of these stations are shown in Fig. 5. In addition, DMI has developed a 10-km gridded precipitation product (Scharling et al., 2006) based on spatial interpolation of dynamically corrected gauge observations.

The DMI is currently operating seven climatic stations in and close to the Skjern catchment (Fig. 5). At these stations, the following variables are measured and reported at 1-h resolution: incoming shortwave radiation, wind speed, relative humidity, air temperature, and air pressure. Standard meteorological equipment is used at these seven stations. The data recorded at these stations are further used for developing 20-km gridded products.

Within the catchment, 11 streamflow gauging stations functioning (Fig. 5) and operated by the Danish Center for

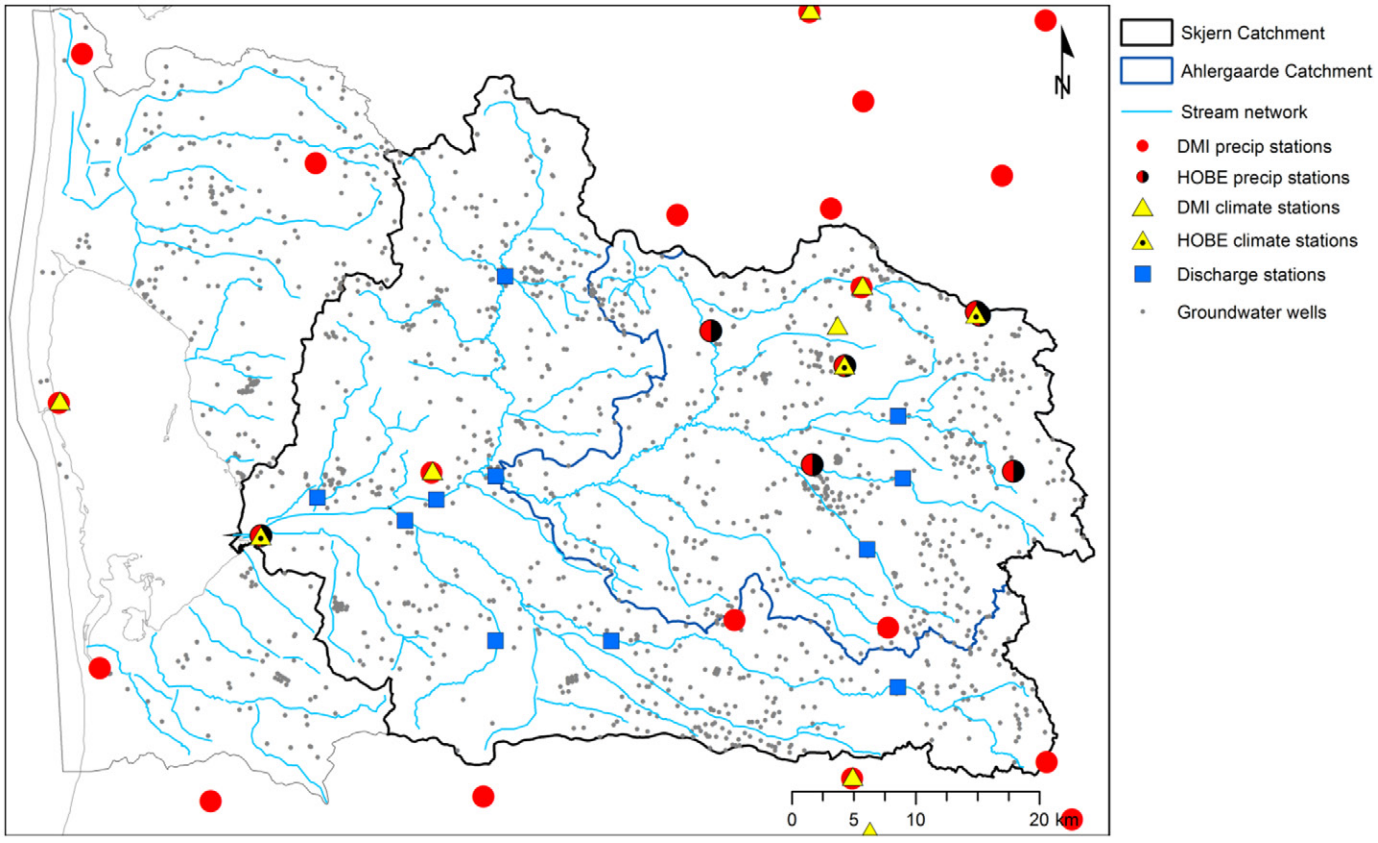

Fig. 5. Discharge, precipitation, climatic stations, and groundwater observation wells.

Environment and Energy. Mean hourly discharge is estimated using a standard method, where seasonal rating curves are used to convert observed water levels to discharge rates. One of the stations (Ahlergaarde) has an observation record dating back to 1920.

Observations of hydraulic head are available from about 3000 wells within the Ringkøbing Fjord area (Fig. 5). These observations are retrievable from the Jupiter database maintained by the Geological Survey of Denmark and Greenland (http://www.eng.geus.dk/products-services-facilities/data-and-maps/national-well-database-jupiter/). For some wells sporadic time series are available, whereas for others only one measurement is reported, often at the time of well construction.

Within the entire area, 834 abstraction wells for domestic and industrial water supply and 4754 abstraction wells for irrigation are registered. No reliable data exist for the abstraction rates for irrigation. Farmers are typically allowed to irrigate up to 100 mm yr^{-1} on irrigated land, which amounts to about one-third of the catchment area. The actual area of irrigation taking place varies from year to year and depends on cropping rotation and the prevailing climate. Stisen et al. (2011) estimated that mean annual irrigation is 15 to 30 mm yr^{-1} for the entire area and 45 to 90 mm yr^{-1} for the irrigated areas.

Selected Results

Figure 6 shows the regional distribution of bias-corrected mean annual precipitation for the period 1990 to 2014 based on the grid product from DMI. The highest precipitation occurs in a north–south corridor through the middle of the catchment (~1100 mm yr^{-1}) and with smaller amounts toward the east and west (~900 mm yr^{-1}) (Fig. 6).

Table 2 lists the overall mean annual water balance components for the years 2001 to 2014 based on model simulations by the MIKE SHE model for the Ahlergaarde catchment (Stisen et al., 2011). Precipitation is distributed roughly equally between discharge and ET (Table 2). The overland flow contribution to streamflow is very small because this only occurs in the wetlands where the groundwater table is close to the ground surface. Baseflow and drainage flow are the two main contributors. The latter component represents flow through surface and subsurface drainage systems as well as the lateral flow in the near subsurface with a shorter response time than the baseflow component. Subsurface drain installations are widely used in Denmark to improve agricultural cultivation and crop growth conditions, and they have a major impact on the rainfall–runoff relationships. The overall hydrological conditions of the catchment represent a temperate stream system mainly fed by subsurface water.

Figure 7 shows time series for 2014 for the Ahlergaarde catchment of measured precipitation, computed potential ET using the Penman–Monteith equation, as well as model-computed actual ET, recharge, pumping for water supply/irrigation, and discharge components. Precipitation occurs throughout the year, although

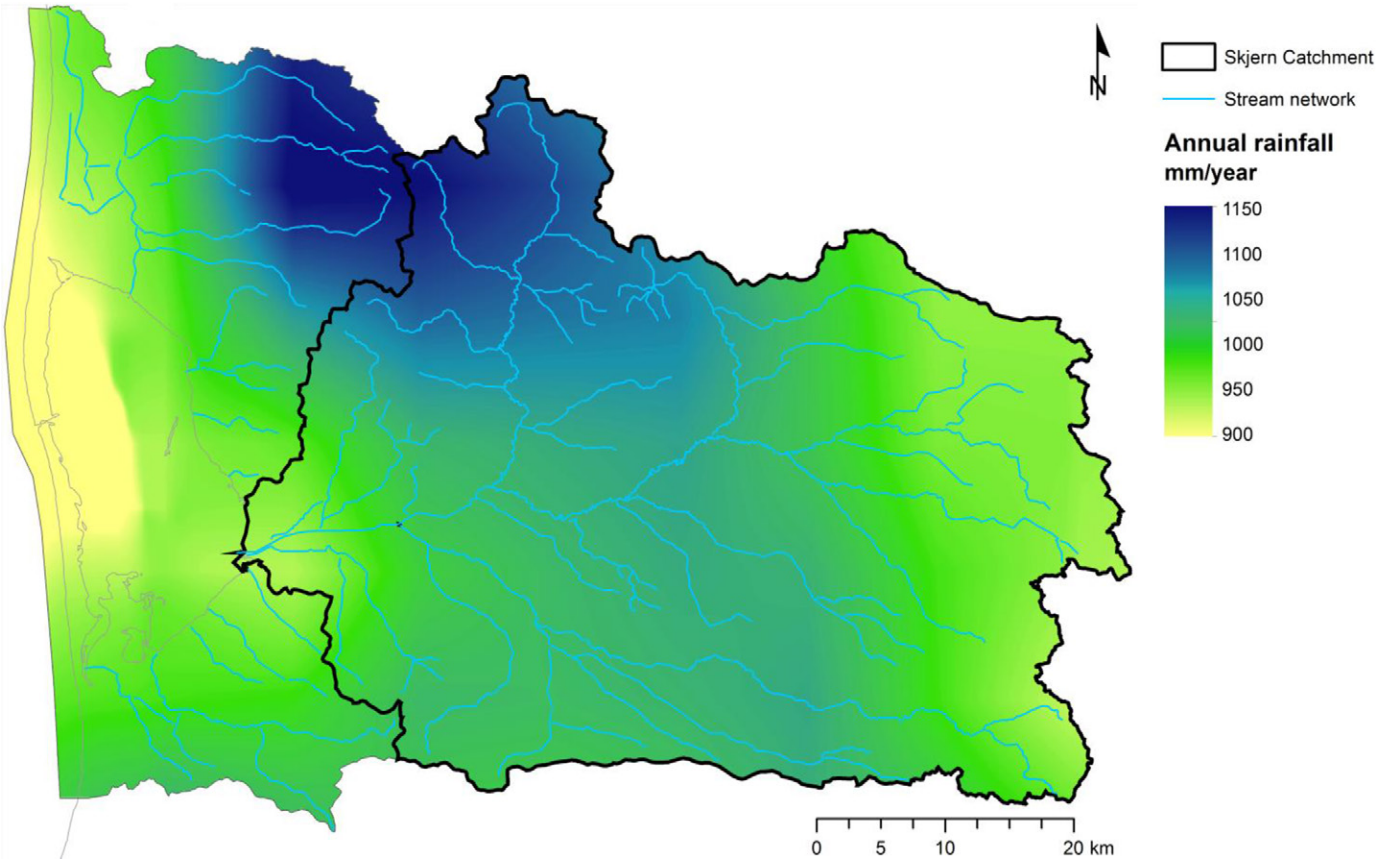

Fig. 6. Regional variation of mean annual precipitation for the period 1990 to 2014.

Table 2. Mean annual water balance components for the Ahlergaarde subcatchment (1050 km^2) for the period 2001 to 2014 based on MIKE-SHE model simulations (Stisen et al., 2011).

Variable	Avg. 2001–2014
	mm yr^{-1}
Precipitation	1053
Potential evapotranspiration	618
Actual evapotranspiration	495
Recharge	558
Overland flow to stream	11
Drainage flow to stream	206
Baseflow to stream	266
Stream flow	483
Groundwater flow across model boundary	53
Storage change	22

precipitation is typically higher in late summer, autumn, and winter (Fig. 7). The highest potential ET occurs during the summer, where the difference between potential and actual ETs is highest due to water stress in the root zone. Groundwater recharge occurs mainly in late autumn, winter, and early spring. Most pumping takes place during summer due to widespread irrigation of the agricultural fields. For 2014, pumping for water supply and irrigation was 12 and 55 mm yr^{-1}, respectively. The river discharge time series shows seasonality, with highest discharges during winter. It is a perennial stream system, and the relatively high values during summer are due to groundwater inflow, which exhibits a small seasonal variation.

Dedicated Observations

A series of dedicated observations and measurement campaigns have been performed in the observatory exploiting recent developments in instrumentation and sensor technologies. Some of these are illustrated in Fig. 8. Observations and measurement campaigns have been performed to address specific research questions and to provide new data for analyzing water balance closure at various spatial scales.

Data Collection

Agricultural Field Observatory

Six local field observatories have been established within the HOBE hydrological observatory (Fig. 1). At three sites representing agriculture, coniferous forest, and meadow grassland, detailed climatic and subsurface measurements are performed.

The most comprehensive data collection is taking place at the agricultural site. Table 3 lists the variables being measured, number of stations, start of measurements, and temporal resolution.

The site is equipped with seven precipitation gauges produced by different manufacturers. One 200-cm^2 OTT Pluvio2 automatic rain gauge has been installed in a pit covered by a metal grid and with the orifice at ground level to avoid turbulence effects. The other gauges have been installed at different heights and with different wind protection measures. One of the gauges is protected by a double fence according to World Meteorological Organization guidelines for measurement of liquid precipitation (Goodison et al., 1998).

Standard climatic variables, including radiation components, wind speed, wind direction, temperature, and relative humidity, are measured using standard instrumentation installed at 4-m height in a 12-m-tall flux tower. In addition, the weather type is measured by two distrometers (Thiess Instruments).

The 12-m flux tower is in an area surrounded by agricultural fields. On the top of the tower, a sonic anemometer (R3–50, Gill Instruments Ltd.) has been mounted, with gas inlets connected to a CO_2/H_2O analyzer (LI-7000, LI-COR). Two soil heat flux plates at 5 cm depth measure the heat flux in the soil. Details of the energy flux measurements are described in Ringgaard et al. (2011). An additional tube inlet is connected to a N_2O analyzer (Herbst et al., 2011). Data are collected at 10 Hz and connected to a data logger for subsequent transfer to a server. The data are processed using the AltEddy software package (Alterrra, Univ. of Wageningen) and aggregated to half-hour fluxes. Gap filling is performed using the method adopted by CarboEurope and FLUXNET (Moffat et al., 2007).

A large number of soil moisture sensors were installed at the site, including TDR probes and Decagon 5TE capacitance probes, and connected to dataloggers for automated recording. The probes were installed in replicates at different depths, and the TDR probes have different shapes and vertical extent (see Vasquez [2013] for details). Additionally, a few soil tensiometers and suction cups were installed.

Two CR1000B cosmic ray probes (Hydroinnova) were installed at the site. One detector is a bare detector filled with proportional gas for measurement of thermal neutrons. The other moderated detector is shielded with plastic for measurement of epithermal neutrons (Andreasen et al., 2016). The moderated detector is suitable for providing estimates of soil moisture for a footprint of 500 to 600 m in diameter and for a depth ranging from typically 40 to 70 cm. Thus, soil moisture measurements by the cosmic ray technique represent a much larger support volume than traditional soil moisture probes and are in better accordance with typical grid elements in a distributed hydrological model.

A lysimeter facility was established consisting of four tanks made of black polyethylene with welded seams for collection of recharge water. After excavation, each of the tanks was installed with an open surface area of 3.2 by 3.88 m at 0.6 m depth. The installation at depth facilitates normal agricultural activities. The depth of the tanks is 1.1 m at one side and 1.5 m at the other. The bottom of each tank has a sloping face of 10.3% along the 3.88-m side to facilitate collection of recharge water with minimal buildup of a water table. At the deepest end of each tank, a perforated tube collects the percolated water, which is diverted to a collection well, where the flow from each tank is measured by a tipping bucket gauge. After installation, the tanks were backfilled in the same order as the parent material. After backfilling, nine 1-m-long TDR probes were installed vertically over a depth interval of 0.6 to 1.6 m

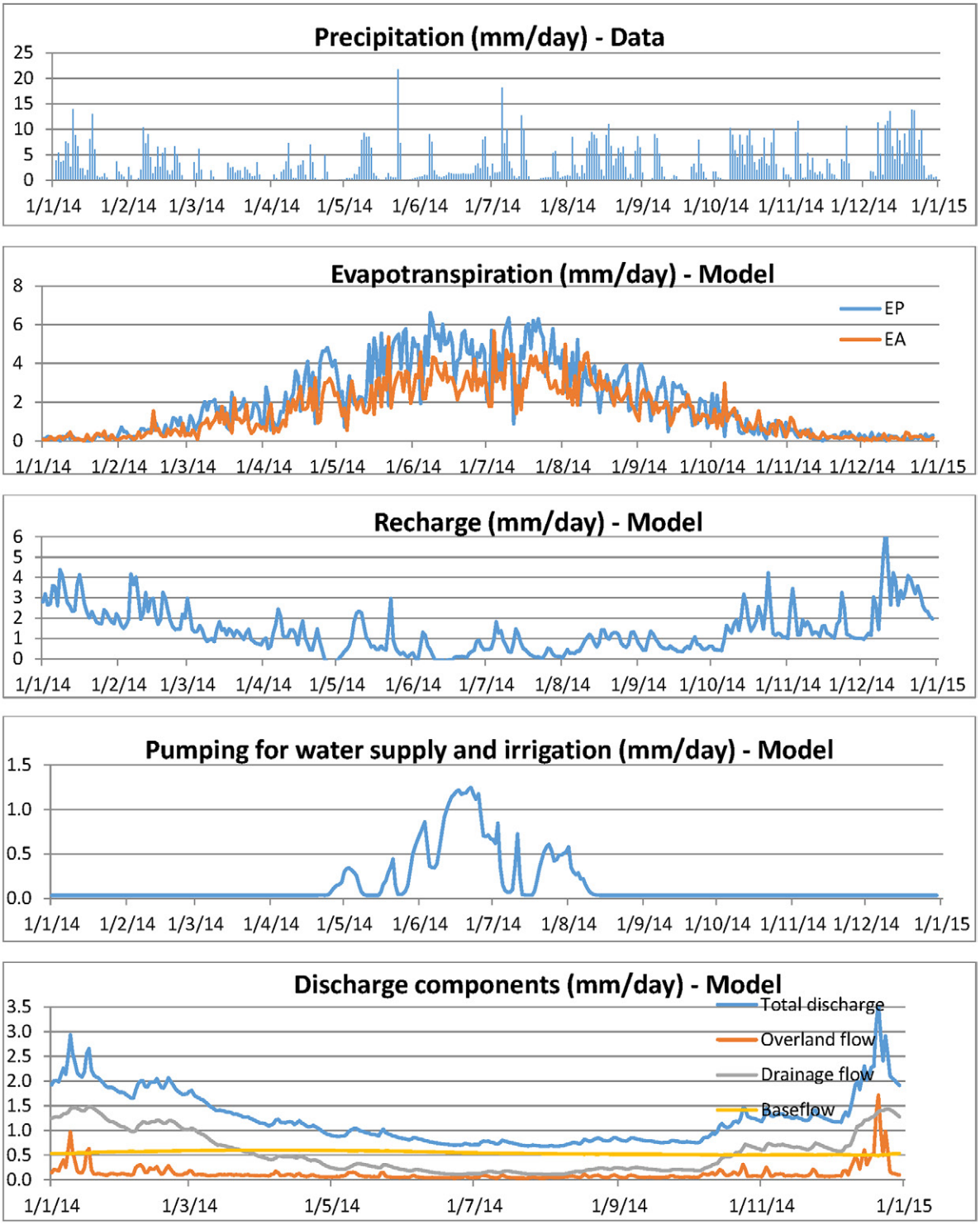

Fig. 7. Daily values for year 2014 for the Ahlergaarde catchment; (a) precipitation; (b) potential and actual evapotranspiration; (c) recharge; (d) irrigation; and (e) discharge.

in each tank to measure water content. All probes were connected to a multiplexed TDR instrument. Finally, the tanks were covered by 60 cm of the original soil material. The experimental setup is described in more detail in Vásquez et al. (2015).

Hydraulic heads are measured in three shallow wells and in one deep well screened at different levels.

The field site was equipped with two hydrogeophysical arrays Haarder et al. (2015). One is for cross-borehole georadar measurements and consists of four 6-m access tubes. The other is for cross-borehole electrical resistivity measurements and consists of five 6-m tubes with electrodes every 25 cm. Fifteen unpolarizable electrodes were installed for self-potential measurements.

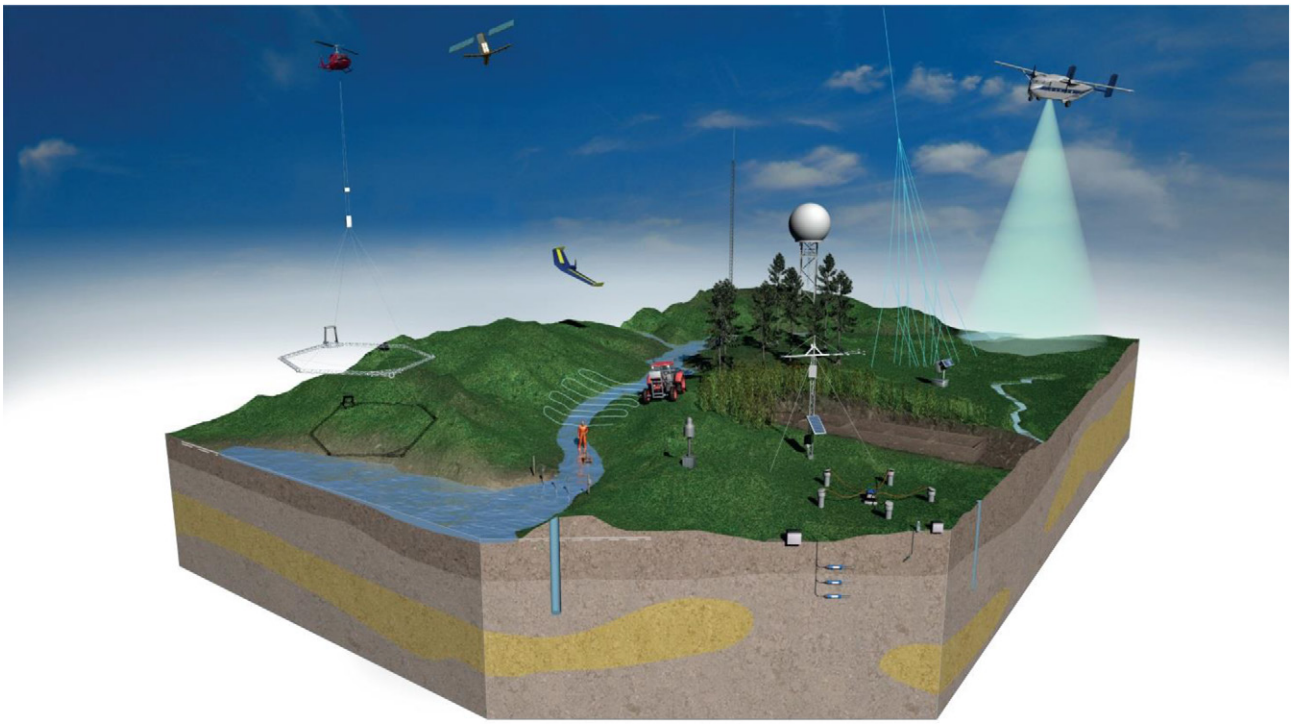

Fig. 8. Illustration of dedicated measurements and campaigns.

Forest Field Observatory

The forest field site is less well equipped than the agricultural site, although it has a flux tower that has a height of 38 m to exceed the height of the forest stands (Table 4).

The same climatic variables are measured at this site as for the agricultural site but at 30 m above the forest floor. Temperature and relative humidity are measured at 15 m as well. Also at this site, the eddy covariance instrumentation consists of a sonic anemometer connected to a CO_2/H_2O analyzer (Ringgaard et al., 2011).

Similar to the agricultural site, automated systems for soil moisture measurements were installed using TDR probes as well as

Table 3. Dedicated observations at the agricultural field observatory.

Variable	No. of devices	Time period	Temporal resolution
Precipitation	seven placed at different heights and with different shielding	2009–present	10 min
Weather type (distrometer)	two	2009–present	10 min
Radiation (net, short wave, long wave)	one	2009–present	10 min
Wind speed and direction	one	2009–present	10 min
Air and soil temperature, humidity	one	2009–present	10 min
Energy fluxes (latent, sensible)	12-m flux tower	2009–present	half hourly
Soil heat flux	two plates at 5-cm depth	2009–present	half hourly
Greenhouse gasses (CO_2, N_2O)	12-m flux tower	2009–present	half hourly
Recharge (underground lysimeters)	four	2009–present	half hourly
Hydraulic head	three shallow wells	2009–present	hourly
Hydraulic head	one deep well with screens 5–7-, 7–9-, 13–15-, and 33–35-m depths	2009–present	hourly
Cosmic ray sensors	two (moderated and bare) at 1.5 m	2013–present	hourly
Soil moisture probes (TDR, Decagon 5TE)	~100 probes at different locations and depths	2009–present	half-hourly
Soil water pressure	~30 probes at different locations and depths	2009–present	half-hourly
Suction cups	four at depths of 1, 2, 3, and 4 m	2009–present	weekly
Cross-borehole georadar array	4- by 6-m access tubes		
Cross-borehole ERT array	5- by 6-m tubes, electrodes placed every 25 cm		
Self-potential electrodes	15 unpolarizable electrodes		

Table 4. Dedicated observations at the forest field observatory.

Variable	No. of devices	Time period	Temporal resolution
Precipitation	one placed in the forest, one in the clearing	2009–present	10 min
Radiation (net, shortwave, longwave)	one	2009–present	10 min
Wind speed and direction		2009–present	10 min
Air and soil temperature, humidity	one	2009–present	10 min
Energy fluxes: latent, sensible	38-m flux tower	2009–present	half-hourly
Soil heat flux	two plates at 5-cm depth	2009–present	half-hourly
Greenhouse gasses (CO_2)	38-m flux tower	2009–present	half-hourly
Hydraulic head	two shallow wells	2009–present	hourly
Cosmic ray sensors	two (moderated and bare) at 1.5 m	2013–present	hourly
	two (moderated and bare) at 27.5 m	2013–2015	
Soil moisture probes (TDR, Decagon 5TE)	~40 probes at different locations and depths	2009–present	half-hourly
Soil water pressure	10 probes at different locations and depths	2009–present	half-hourly
Throughfall	four guttering collector systems	2010–2011, 2013–present	half-hourly
Stemflow	four stems	2010–2011	half-hourly
Sapflux	four stems	2010–2011	half-hourly

Decagon water content and suction sensors. Details can be found in Vasquez (2013).

One set of cosmic ray sensors (bare and moderated detectors) was installed at 1.5 m height. Another set was in operation at 27.5-m height for a short period.

Throughfall was measured by simple buckets and guttering systems, and campaigns with stem flow and sapflux measurements were conducted (Ringgaard et al., 2014).

Meadow Grassland Field Observatory

This site is located at the outlet of Skjern River next to a brackish lagoon. The site represents a wetland with low grass vegetation and a shallow groundwater table. As for the other two field observatories, basic climatic and hydrological variables are measured in the form of soil moisture, soil water pressure, and water table level (Table 5).

A 7-m flux tower was installed, onto which climatic sensors and eddy covariance instrumentation were mounted. Measurements of CO_2/H_2O and CH_4 are performed (Ringgaard et al., 2011).

Heathland Field Observatory

The heathland field observatory is a marginally instrumented site compared with the other field sites because only one moderated cosmic ray sensor has been installed together with six Decagon 5TE stations, each having five sensors at three depths (Table 6).

Table 5. Dedicated observations at the meadow grassland field observatory.

Variable	No. of devices	Time period	Temporal resolution
Precipitation	one	2009–present	10 min
Radiation (net, short wave, long wave)	one	2009–present	10 min
Wind speed and direction	one	2009–present	10 min
Air and soil temperature, humidity		2009–present	10 min
Energy fluxes (latent, sensible)	7-m flux tower	2009–present	half-hourly
Greenhouse gasses (CO_2, CH_4)	7-m flux tower	2009–present	half-hourly
Soil heat flux	two plates at 5-cm depth	2009–present	half-hourly
Hydraulic head	two shallow wells	2009–present	hourly
Soil moisture probes (TDR, Decagon 5TE)	~40 probes at different locations and depths	2009–present	half-hourly
Soil water pressure	five probes at different depths	2009–present	half-hourly

Table 6. Dedicated observations at the heathland field observatory.

Variable	No. of devices	Time period	Temporal resolution
Cosmic ray sensors	one moderated and bare at 1.5 m	2014–present	hourly
Soil moisture probes (Decagon 5TE)	six stations with five sensors: two sensors at 2.5 cm, two sensors at 22.5 cm, one sensor at 52.5 cm	2014–present	half-hourly

Field Observatories for Groundwater–Surface Water Flow Exchange

At these sites, flow exchange between two types of water bodies is measured using a series of piezometers and temperature probes. These measurements are supplemented by grab water samples for stable isotope measurements. Details can be found in Jensen and Engesgaard (2011), Karan et al. (2013), and Sebok et al. (2015).

Soil Moisture and Temperature Network

Within the Ahlergaarde catchment, a network of 30 soil moisture stations was established for continuous measurements of soil moisture, temperature, and electrical conductivity (Fig. 9). At each location, Decagon 5TE capacity sensors were installed at depths of 5, 20, and 50 cm and connected to dataloggers for measurements at 30-min intervals (Table 7). An additional sensor was installed in the organic surface layer at sites with natural vegetation. The network was designed to provide a representative coverage of land cover, soil type, and precipitation conditions. Stations located in agricultural fields are temporarily removed twice a year to allow for cultivation of the fields and then later reinstalled. This leads to gaps in the data series. Details on the soil moisture network can be found in Bircher et al. (2012b).

Groundwater Diver Network

A network of nine wells with pressure transducers installed (Eijkelkamp mini divers) was established within the Ahlergaarde catchment to provide bi-hourly measurements of groundwater heads (Fig. 9) (Ridler et al., 2017).

Isotope Network

A network of five stations for measuring isotope concentrations in precipitation was established (Fig. 9) (Müller et al., 2017).

Selected Results

Figure 10 shows daily values of local climatic and hydrological variables for 2014 from the agricultural field observatory. The seasonal variation of the local climatic variables follows largely the variation in areal values for the Ahlergaarde catchment shown in Fig. 7. Estimated potential ET is generally higher or equal to measured actual ET based on eddy covariance observations. Prior to the main growing season starting in April, actual ET is less than potential ET because no irrigation takes place. In the main growing season (May to mid-July), extensive irrigation brings actual ET to the level of potential ET, which on some days may reach 6 mm d^{-1}. After harvest in mid-July, actual ET is reduced to low values.

The average soil moisture over the upper 50 cm has a relatively small seasonal variation, with the lowest values during the summer. This variable is highly influenced by irrigation. Outflow from the lysimeters mainly occurs in autumn and winter. The local values are at times higher than the areal values, which can be expected because the areal values represent spatial averages for the entire

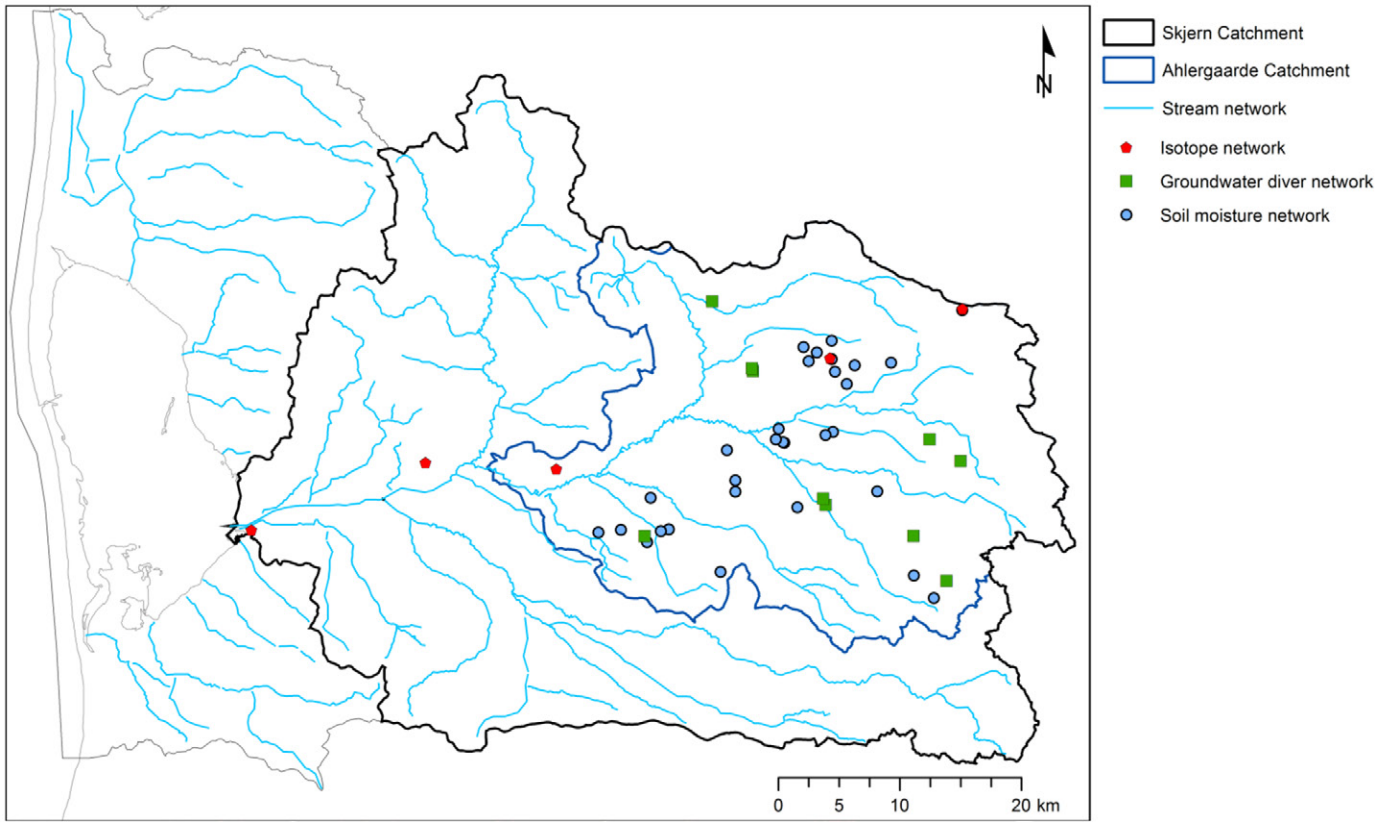

Fig. 9. Soil moisture, groundwater, and isotope network.

Table 7. Measurement network in the Ahlergaarde catchment.

Network	Variable	No. of stations	Time period	Temporal resolution
Soil moisture network	soil moisture, temperature, electrical conductivity	30 (depths 5, 20, 50 cm)	2009–present	half-hourly
Groundwater diver network	hydraulic head	10	2012–present	hourly
Rainfall isotope network	isotope concentration	5	2012–present	monthly

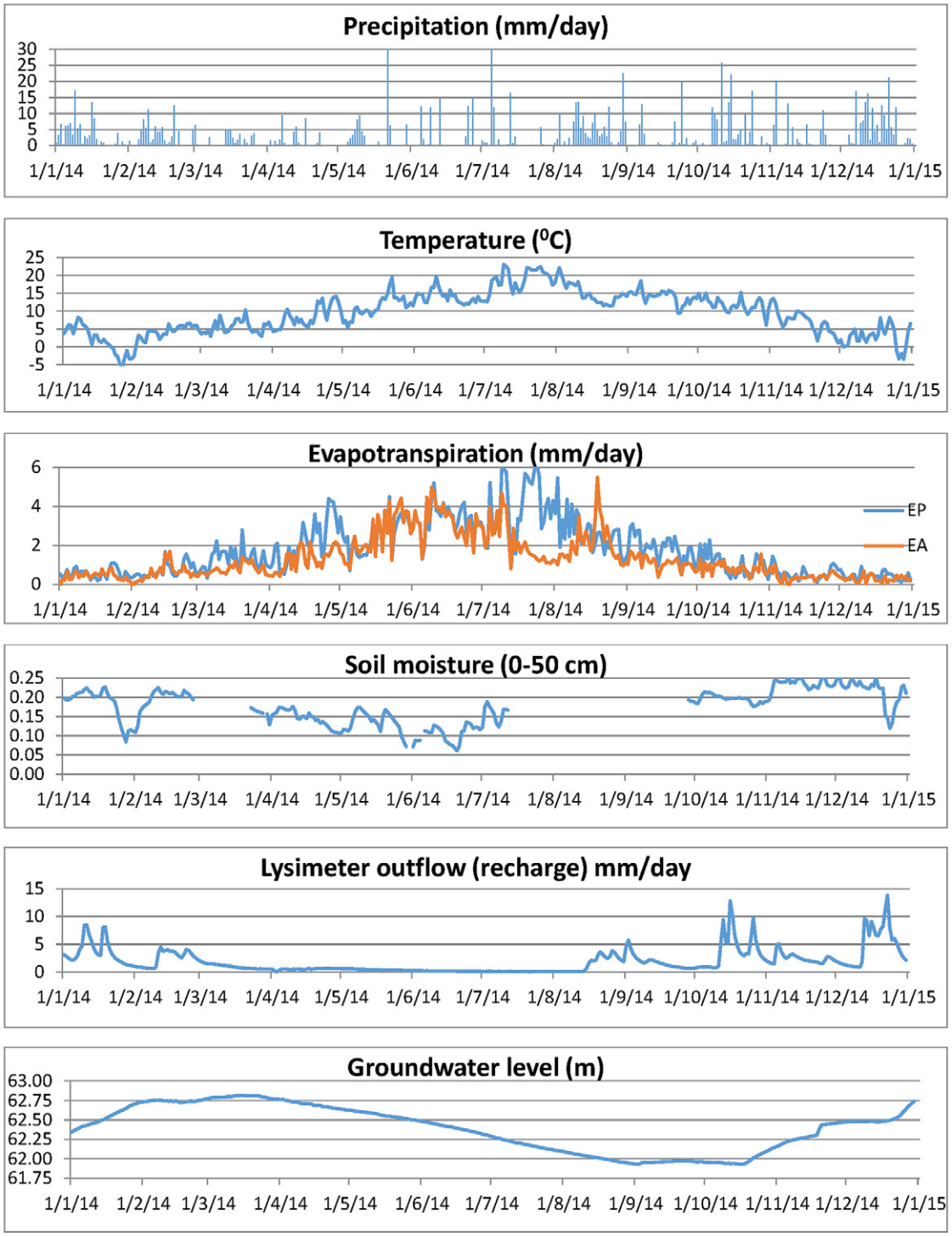

Fig. 10. Daily values for 2014 at the agricultural field observatory: (a) precipitation; (b) air temperature; (c) potential evapotranspiration based on the Penman–Monteith equation and actual evapotranspiration based on flux measurements; (d) soil moisture (mean, 0–50 cm); (e) recharge; and (f) groundwater level.

catchment. During summer, the local recharge values are almost zero, whereas recharge pulses occur at the catchment scale due to heterogeneity in hydrologic properties within the catchment. The highest groundwater table occurs in March and April.

Figure 11 shows daily values for 2014 of cosmic ray-derived soil moisture for the three different land-cover sites where cosmic ray sensors were installed. The values for agriculture and forest have the same magnitudes and seasonal variation, whereas the values for heathland are higher because the soil at this location has higher water retention and the groundwater table is higher. Overall, the observations reflect the seasonality in climatic conditions. Values for the agricultural site are in reasonable accordance with the values shown in Fig. 10.

In Fig. 12, results from the soil moisture network are shown as averaged values and standard deviation at three depths for year 2014. Slightly higher seasonal variations are observed for the upper two levels, reflecting that the vegetation mostly affects these levels. Generally, a higher spatial variation is observed at the lowest level because soil moisture here is affected by the presence of a hard pan at some locations (Andreasen et al., 2013). Generally, the spatial variation is larger during autumn and winter than during spring and summer.

The eddy covariance results for energy fluxes at the local sites were used for calibration of the integrated hydrological model as described below. The data from the soil moisture network were used for validation of remote sensing products as well as for assimilation and calibration of integrated hydrological modeling.

Soil moisture estimates from cosmic ray neutron measurements were applied for assimilation and calibration.

Dedicated Experiments and Campaigns

Several dedicated experiments and campaigns have been performed in the HOBE observatory, all contributing to addressing the research questions highlighted above. Below, a few selected activities are described.

Groundwater–Surface Water Interaction

At several stream sections along the Holtum Stream,tributary, piezometers and wells have been established for hydraulic measurements and water sampling for stable isotopes, age dating, and chemical analysis. Temperature has been used as a tracer for estimating the fluxes between the hydrological compartments measured either in vertical profiles by probes (Duque et al., 2016; Jensen and Engesgaard, 2011; Karan et al., 2013, 2017) or as distributed sensing (Sebok et al., 2013, 2015; Frederiksen, 2017).

Figure 13 shows an example of a temperature measurement campaign for detailed mapping of the exchange of water across a section of a riverbed. In this example, 40 probes were installed in an array covering 40 m^2 with a lateral spacing of about 1 m and with 10 temperature sensors on each probe with variable vertical spacing. The sensors were connected to dataloggers for automated logging of the temperature (Karan et al., 2014). Figure 13b shows the location of the probes, and Fig. 13c shows the three-dimensional variation of temperature in the streambed for a particular day, highlighting the variation in temperature contrast between stream water and groundwater.

Environmental tracers (Karan et al., 2013) and stable isotopes (Müller et al., 2017; Poulsen et al., 2015) have also been used for investigating fluxes between groundwater and surface water.

Dedicated measurements have been performed along lake shorelines (Sebok et al., 2013) and along the shoreline of the coastal lagoon near the outlet of Skjern River (Duque et al., 2016).

An airborne geophysical campaign was performed over the brackish Ringkøbing lagoon located next to the North Sea and the recipient of the discharge from Skjern River (Kirkegaard et al., 2011). An airborne time domain electromagnetic system (AEM) was used for mapping the freshwater/brackish water distribution beneath the lagoon bed. Submarine groundwater discharge takes

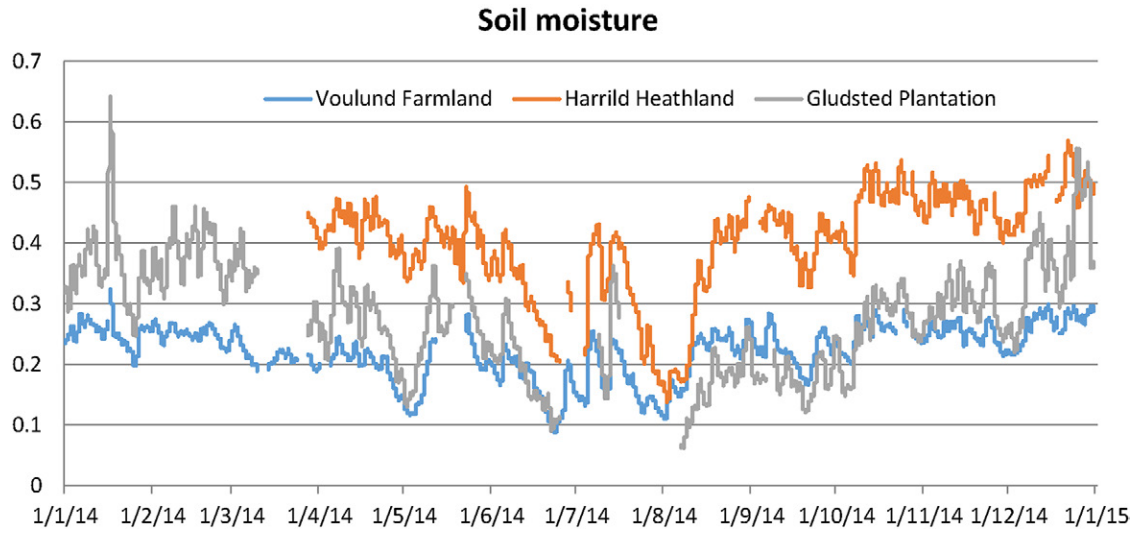

Fig. 11. Daily values for soil moisture derived from the cosmic ray method.

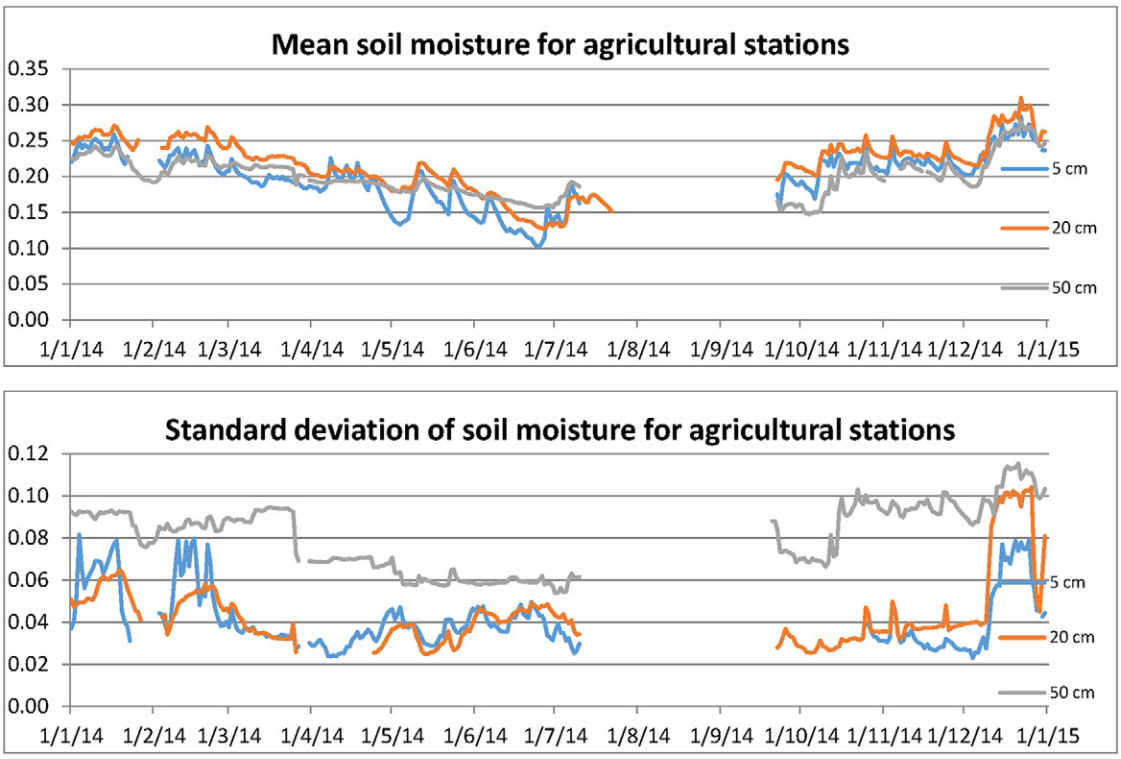

Fig. 12. Daily average values and standard deviation of soil moisture at three depths for the agricultural stations from the Ahlergaarde soil moisture network.

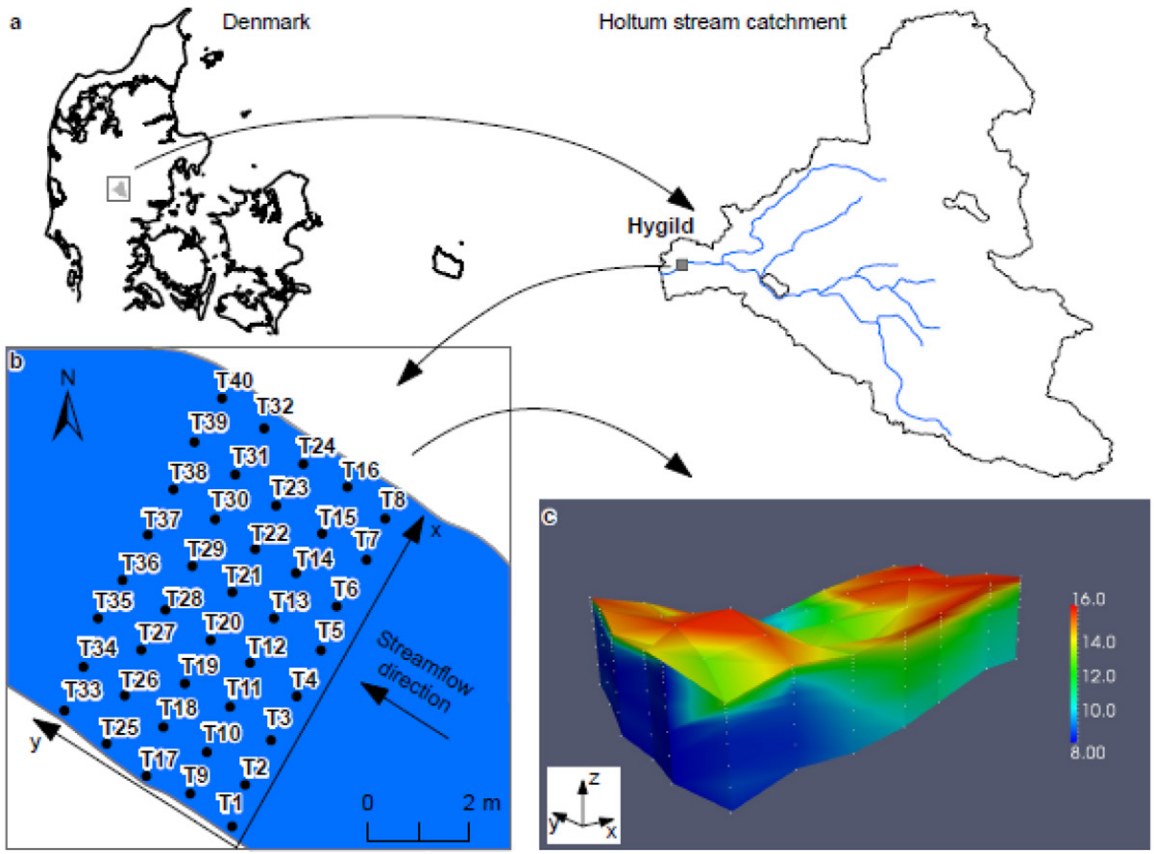

Fig. 13. (a) Location of the temperature probe setup in a tributary to the Skjern River, (b) location of 40 temperature probes, and (c) three-dimensional view of mean daily temperature 1 July 2010 (vertical axis exaggerated three times) (reproduced from Karan et al., 2014).

place in the lagoon, and the overall purpose of the campaign was to map the salinity distribution of the coastal aquifer to provide data for constraining a numerical model and thereby quantifying the groundwater outflow (Haider et al., 2015). Figure 14a shows two flight lines over the lagoon, and Fig. 14b shows the derived resistivity distribution in two cross-sections as well as the delineation of groundwater flow pathlines and the freshwater–brackish water interface.

The air-borne system was further used for mapping the geological settings in the northern part of the catchment (He et al., 2017). The AEM technology is an efficient noninvasive technique to map the subsurface settings over large areas, and it has been widely used in Denmark (Sørensen and Auken, 2004).

Airborne Campaign with L-Band Radiometer

An airborne campaign with the L-band radiometer EMIRAD-2 was performed within one Soil Moisture and Ocean Salinity (SMOS) pixel (44 by 44 km) (Kerr et al., 2001) in the HOBE catchment to obtain data on brightness temperatures (Bircher et al., 2012a). The flight campaign was carried out for validation of SMOS data under Danish climatic conditions. At the same time, soil and vegetation samples were collected for obtaining ground truth data (Fig. 15).

Tracer Experiments at the Agricultural Field Observatory

A tracer experiment was performed at the agricultural field observatory using saline solution as tracer. The tracer was added to the surface, and the tracer migration was monitored using cross-borehole electrical resistivity tomography (ERT) from boreholes installed to 6 m depth (Haarder et al., 2015).

Another tracer experiment was performed using bromide as a tracer. Concentrations in the soil water were measured in water samples extracted from suction cups installed at depths of 1, 2, 3, and 4 m (Vasquez, 2013).

Unmanned Aerial Vehicle Surveys

Flight campaigns for mapping crop water stress and for estimating energy fluxes for an area near the agricultural field observatory were performed using an unmanned aerial vehicle (UAV) with a thermal infrared camera and a camera for detecting energies in the red, green, and blue bands on board (Hoffmann et al., 2016a, 2016b).

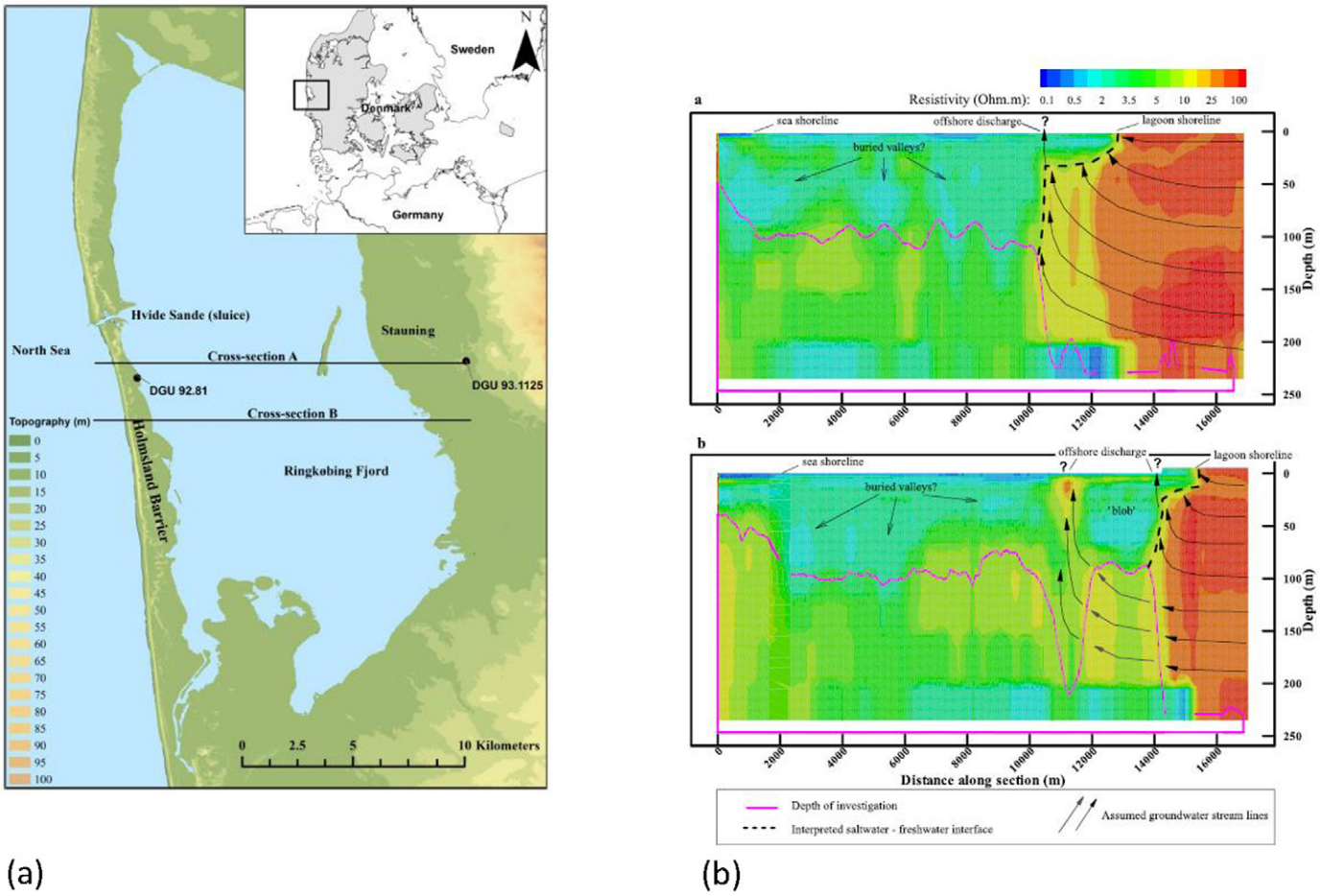

Fig. 14. (a) Two selected geophysical survey lines across Ringkøbing lagoon and (b) two-dimensional resistivity inversion profiles. Solid lines represent assumed groundwater flow lines, dashed lines represent assumed brackish water–groundwater interface, and assumed zones with offshore submarine groundwater discharge are marked as "?" (reproduced from Haider et al., 2015).

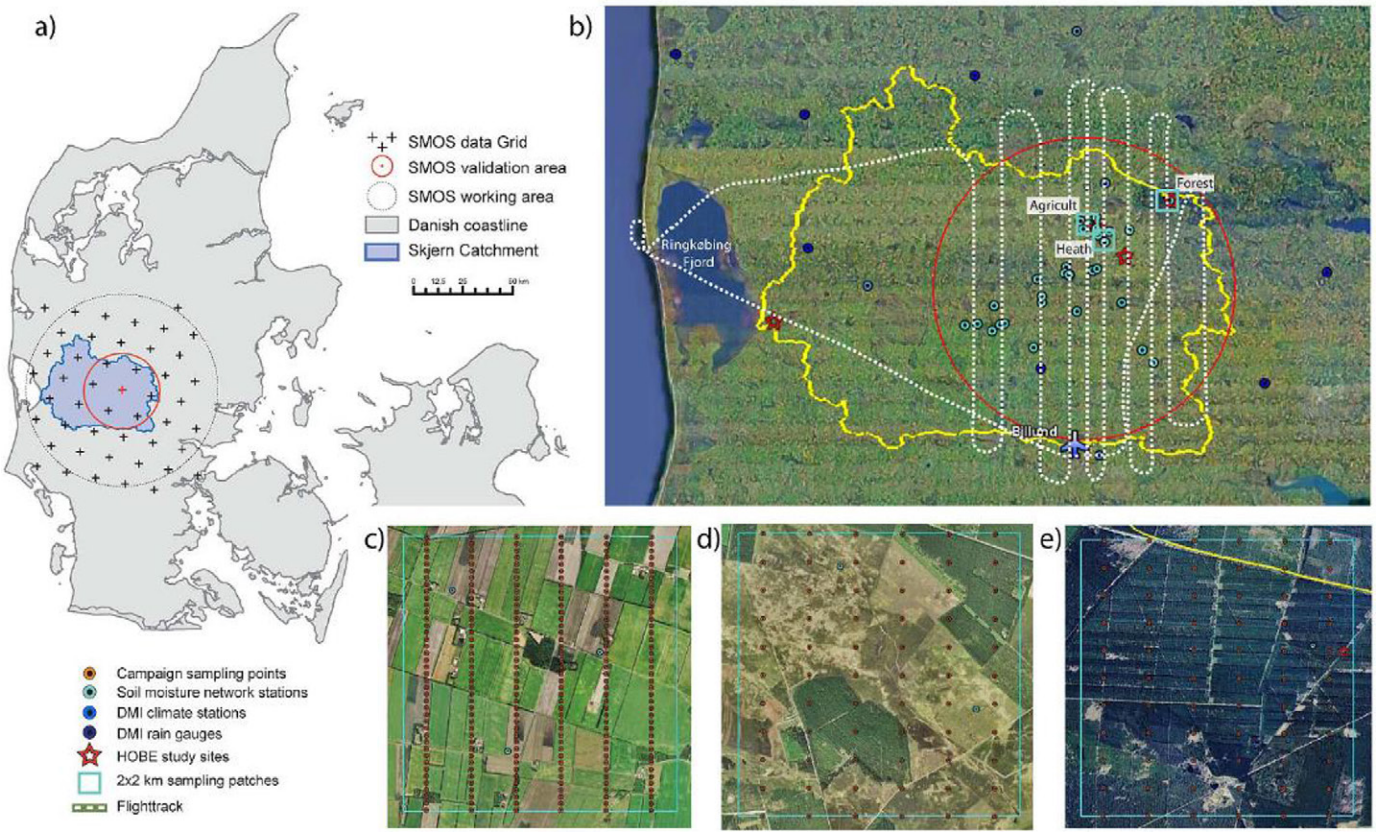

Fig. 15. Flight campaign with L-band radiometer over the Skjern catchment: (a) location of the validation SMOS pixel; (b) flight tracks; (c) sampling locations near the agriculture field observatory; (d) sampling locations near the heathland field observatory; and (e) sampling locations near the forest field observatory (reproduced from Bircher et al., 2012a).

Data Management and Policy

All relevant historical data, including spatial data (surface elevation, geological characterization, vegetation classification, and soil classification) and time series (meteorological, hydrological, and hydrogeological) are stored in a database developed with a user-friendly interface for easy retrieval. Data generated as part of the HOBE project are also retrievable from the database. The database facilitates easy data sharing among scientists and students affiliated with HOBE and dissemination of data to interested national and international parties. Access to data is granted for research purposes and on signing a user statement. Information about retrieval of data can be found at http://www.hobecenter.dk/. The data can also be accessed through the data portal of the European Network of Hydrological Observatories (ENOHA; https://enoha.eu/). We recommend that interested parties consult the data providers before use in order obtain detailed information on how data were collected and processed.

Data from the soil moisture network are available through International Soil Moisture Network Database (https://ismn.geo.tuwien.ac.at/) and the European Centre for Medium-Range Weather Forecasts (https://www.ecmwf.int/).

Modeling

The integrated and distributed modeling system MIKE SHE (Abbott et al., 1986) has been the system of choice for catchment-scale modeling activities. The modeling system has been used for making an integrated and coherent interpretation of the data collected in the HOBE observatory, for hypothesis testing, and for analyzing the validity of various precipitation, evapotranspiration, and remote sensing products.

A two-way coupling between the climate model HIRHAM and MIKE SHE has been developed, allowing for feedback processes between the land surface and the atmosphere (Larsen et al., 2014, 2016a).

Data assimilation methods for MIKE SHE have been developed and tested. Rasmussen et al. (2015) applied ensemble Kalman filtering for parameter estimation by assimilating groundwater head and discharge observations. They found improvements in parameter estimation when applying an adaptive localization technique and when increasing the ensemble size. Bias-aware data assimilation methods in integrated hydrological modeling were analyzed using Ensemble Transform Kalman Filtering (Rasmussen et al., 2016; Ridler et al., 2017), and the effect of ensemble size

and localization and the impact of uncertainty on the filter performance were tested (Rasmussen et al., 2015; Zhang et al., 2015). Multivariate data assimilation of soil moisture and groundwater head was analyzed by Zhang et al. (2016), who found relatively weak correlations between surface soil moisture and groundwater head through assimilation. Although neither discharge nor ET was included in the filter state vector due to the integrated modeling approach, discharge was improved when head was assimilated, and ET was improved when soil moisture was assimilated.

Other types of model codes have been applied to study individual hydrological compartments or exchange processes, including MODFLOW (He et al., 2013a, 2014), FEFLOW (Müller, 2016), HydroGeosphere (Haider et al., 2015; Karan et al., 2013), HYDRUS (Haarder, 2014), and two-source energy balance models DTD/TSEB (Guzinski et al., 2013; Hoffmann et al., 2016b).

New Insights and Novel Scientific Findings

Many of the new insights and scientific findings obtained in HOBE for the individual hydrological compartments have been attained by integrating results and findings from other compartments, which has been possible due to the integrated nature of the project activities.

Precipitation

Fu et al. (2011) analyzed the impact of the spatial resolution of precipitation on the hydrological response of the distributed and integrated hydrological model MIKE SHE. Six precipitation products of different spatial resolutions were tested in the model. The results showed that the spatial resolution of precipitation had no impact on simulated streamflow at the outlet of the catchment. However, at subcatchment scale the choice of precipitation product made a difference. Even more impact was seen on the simulation of the temporal and spatial variation of groundwater recharge and groundwater head. These findings were in line with the results reported by He et al. (2011), who used weather radar data (C-band Doppler radar) for quantitative precipitation estimation based on a distance-dependent areal estimation method that merges radar data with rain gauge data. This product and precipitation rates based entirely on data from ground-based precipitation gauges were used as input to the MIKE SHE model for comparison of simulation results. The results showed that many more spatial details were present in the simulations based on weather data. The refined spatial resolution was important for the simulation of streamflow in subcatchments <400 km^2, and simulated groundwater recharge was also sensitive to the precipitation product. These results were further substantiated by He et al. (2013b), who clearly demonstrated that radar data have advantages over traditional rain gauge data when simulating the spatial distribution of hydraulic head. He et al. (2018) compared rainfall products based on rain gauge, single-polarization, and double-polarization radar data, and the model performance was tested using the different model forcings.

Stisen et al. (2011, 2012) tested how different methods for correcting precipitation bias affected the model-simulated hydrological response. Due to wind-induced turbulence around the opening of rain gauges, measurements are subject to systematic bias (undercatch), particularly for small raindrops and snow (Allerup and Madsen, 1980). Various methods have been proposed for correction of the precipitation data. Until recently the most common method was based on mean monthly correction factors (Allerup et al., 1998). With a more refined method, referred to as "dynamic correction," the correction factors are computed on a daily basis for either liquid or solid precipitation (Allerup et al., 1997). The correction for liquid precipitation is a function of wind speed and precipitation intensity, whereas the correction for solid precipitation is a function of wind speed and temperature. Stisen et al. (2011, 2012) found that much more physically realistic simulations of the various hydrological processes and better closure of the water balance were obtained when applying a dynamic bias correction.

Evapotranspiration

Ringgaard et al. (2011) analyzed energy fluxes above the three most important vegetation types (forest, meadow, and agriculture) within the Skjern catchment based on eddy covariance measurements. The results documented differences in the seasonal variation in the energy budget for the three surfaces. The forest received more energy than the other sites; however, this was not reflected in the observed latent heat flux, which was found to be strongly dependent on the interception evaporation. For dry surface, the stomatal control was a limiting factor for latent heat flux. For the agricultural site, the latent heat flux was dependent on crop development. During the growing season, the crop was not subjected to water stress because intensive irrigation took place. The meadow site is located next to the Skjern River, and the water level in the river was an important factor for the latent heat flux from this site.

Ringgaard et al. (2012, 2014) performed detailed measurements at the forest site to separate evapotranspiration in interception, transpiration, and forest floor evaporation. Independent measurements were performed in young open canopy and older mature closed canopy stands of sap flow, forest floor evapotranspiration, throughfall, stemflow, gross precipitation, and ET by the eddy covariance method. The results showed that the canopy structure had a major impact on transpiration because the young open canopy had a transpiration that was 30% higher than for the closed-canopy stands. On the other hand, interception of the closed canopy was higher than for the open-canopy stands (34 versus 31% of the gross precipitation, respectively). Overall, the open canopy had an annual ET that was 7.5% higher than the closed canopy.

Hoffmann et al. (2016b) determined the spatial variation in land surface temperature over a barley field at selected days using a UAV with a thermal camera on board. The thermal pictures were converted to high-resolution mosaics, which were used as boundary conditions for two-source energy balance modeling using the

TSEB and DTD models (Norman et al., 1995, 2000). Simulated net radiation and energy fluxes were compared with measurements from the nearby flux tower. Simulations and measurements compared favorably, suggesting that UAV data can be used for estimating evapotranspiration at high spatial and temporal resolution at field scale.

Guzinski et al. (2013, 2014, 2015) used the same two models for estimating the energy fluxes at local and catchment scales constrained by observations of land surface temperature and vegetation characteristics based on satellite data. At the local scale, the estimates were compared with the eddy covariance measurements at the agricultural and forest sites. For the agricultural site, small bias and high correlation were obtained between simulations and observations. For the forest site, the comparison was less favorable but still encouraging. At catchment scale, the results from the two energy balance models were compared with the results by the hydrological model MIKE SHE. The spatial patterns of the energy fluxes simulated by the two energy balance models were more strongly correlated to each other than when comparing the patterns from each of them with the results obtained by the hydrological model. On the other hand, the temporal variations of ET by the two remote sensing models and the hydrological model were well correlated. These results suggest that remote sensing–based energy balance models can provide useful information for hydrological models.

Soil Moisture

Within the Skjern catchment, soil moisture has been measured and estimated at a range of spatial and temporal scales. Schelde et al. (2011) used point-scale TDR measurements for estimating evapotranspiration. Haarder et al. (2012, 2015) used cross-borehole ground-penetrating radar and ERT for estimating soil moisture at much larger spatial support volume (5–7 m in a lateral direction). In the first of these two hydrogeophysical studies, it was found that two-dimensional ground-penetrating radar tomography was capable of resolving lateral and vertical flow pathways, whereas ERT could not provide the same spatial resolution of the moisture content and associated flow pathways.

The cosmic-ray neutron method offers a unique methodology for providing noninvasive measurements of soil moisture at a spatial scale in between the point scale of the traditional soil moisture sensors such as TDR probes (Schelde et al., 2011) and estimates based on satellite platforms such as SMOS (Bircher et al., 2012a). The measurements and footprint area are sensitive to several environmental factors, including barometric pressure, incoming cosmic radiation, vegetation, organic litter, soil characteristics, and canopy interception (Andreasen et al., 2017a, 2017b). Typical footprint areas are 500 to 600 m diameter, which is comparable to the discretization in a distributed catchment model. Andreasen et al. (2016) showed that the neutron signals measured by neutron probes do not represent clean signals. However, by shielding the probes with cadmium foil it is possible to obtain measurements more comparable to the simulation results obtained by neutron transport modeling. Combining neutron measurements and modeling provides a pathway for separating out the impact of different environmental factors and thereby to obtain more reliable measurements of soil moisture. Andreasen et al. (2017a) demonstrated that the method could be used for measuring other relevant variables, such as biomass.

The HOBE site has been subject to validation experiments of data retrievable from the SMOS mission using the soil moisture and temperature network established in the experimental catchment (Bircher et al., 2012a, 2013). The comparison between the average in situ soil moisture content over 0 to 5 cm and the SMOS-based soil moisture was in line with previous studies showing temporal variations that were comparable but subject to bias. The analysis was based on the SMOS soil moisture Level 2 product; later products have shown a better comparison (S. Bircher, personal communication, 2017). An airborne campaign with the L-band radiometer EMIRAD-2 was performed over the Skjern catchment within one SMOS pixel (Bircher et al., 2012b). The campaign validated SMOS brightness temperature estimates of the selected pixel. During the campaign, ground truth measurements were performed. The SMOS data were corrupted by radio-frequency interference, which complicated the comparison; however, for one of the flying days, the two sets of data showed reasonable agreement.

The data from the soil moisture network have further been used for validating soil moisture products from the Soil Moisture Active Passive (SMAP) mission (Colliander et al., 2018; Reichle et al., 2017). Soil moisture data derived from SMOS have also been used for assimilation in the integrated hydrological and soil–vegetation–atmosphere–transfer (MIKE SHE SW-ET) model (Ridler et al., 2014).

Recharge

The subsurface lysimeters installed at the agricultural observatory enable direct measurements of recharge (Vásquez et al., 2015). Different hydrogeophysical methods have been used for indirect estimation of recharge, and these estimates were in reasonable accordance with the direct measurements (Haarder et al., 2015; Jougnot et al., 2015).

At regional scale, the distributed soil moisture network has been used for recharge estimation (Andreasen et al., 2013). By calibrating the one-dimensional soil–plant—atmosphere model Daisy (Hansen, 2002) against soil moisture data from the soil moisture network and using on-site data on land use and field practices as well as data on textural distribution, recharge and ET were estimated for all 30 soil moisture stations. Because these stations are located according to the distribution of land use, soil characteristics, and precipitation within the Ahlergaarde catchment, the derived fluxes also represent the spatial variability within the catchment and the average of the results represents the catchment-scale recharge. The simulated mean recharge for the catchment was in good agreement with the observed mean stream discharge at the catchment outlet.

Several modeling studies using the integrated and distributed hydrological model MIKE SHE have also provided indirect estimates of the regional and seasonal distribution of recharge (Larsen et al., 2016b; Stisen et al., 2011; Zhang et al., 2016).

Groundwater Flow

Groundwater flow and transport are strongly affected by the architecture of the geological settings and the spatial variability of the hydraulic parameters; the characterizations of both are subject to uncertainty (He et al., 2017, 2015, 2014, 2013a; Koch et al., 2014). He et al. (2013b) applied multiple-point geostatistical simulation techniques to generate geological realizations of the geological architecture based on a specified training image and subject to conditioning by hard data in the form of borehole lithological data and soft data in the form of geophysical data. The geological realizations were subsequently introduced into a groundwater model for calibration of selected parameters. The analysis showed that the uncertainty of the geological conceptualization was as significant as the uncertainty of hydraulic parameters.

Recent developments in high-resolution AEM systems (Auken et al., 2014) offer unprecedented opportunities for detailed mapping of the geological and hydrogeological settings, which is very useful information for groundwater models. He et al. (2014) demonstrated that AEM data can be used both for defining a training image and for soft conditioning data and concluded that this type of information is best used for soft conditioning.

He et al. (2017) modeled a subcatchment of the Skjern River incised by a buried valley system and subject to vertical nonstationarity using multiple-point statistics. Buried valleys are common structures in the Skjern catchment. The study showed that the multiple-point statistics method simulated such nonstationary geological systems.

Groundwater–Surface Water Interaction

Studies of fluxes between groundwater and surface water compartments have been a focal research topic during the lifetime of HOBE. Sebok et al. (2013) demonstrated the use of distributed temperature sensing (DTS) (Selker et al., 2006) for mapping the temporal and spatial changes in temperature on a lake bed and to locate areas of groundwater inflow to a section of the lake. The diurnal variation in temperature at the sediment–water interface was measured using a looped DTS layout, and the data were analyzed based on daily minimum temperature, diel amplitude, and daily standard deviation. The study showed that DTS was able to identify major inflow areas, consistent with the results of other methods; however, the method was not able to identify the detailed spatial variability in inflow patterns.

Sebok et al. (2015) delineated the spatial variability of groundwater inflow zones in a soft-bedded stream using a looped DTS system. Using DTS in soft-bedded streams is complicated by sedimentation and scouring processes, which change the streambed morphology and thus the position of the cables relative to the streambed. These processes introduce anomalies in the temperature signal. The study recommended a combined use of DTS and a survey of changing streambed morphology to separate the influence on the temperature signal from changes in streambed morphology and groundwater inflow zones, respectively.

Karan et al. (2013) analyzed the dynamics of groundwater–stream interaction using a combination of temporal monitoring of temperature in a three-dimensional network of temperature probes installed in the streambed and three-dimensional flow and heat transport modeling. The experimental results documented a substantial heterogeneity in fluxes across the streambed during rainfall-runoff events. The study showed that a three-dimensional approach is needed to accurately describe the transport dynamics. Furthermore, it was shown that a detailed characterization of the hydraulic conductivity of the streambed is needed for an accurate simulation of the temporal and spatial variability of the fluxes.

Hydrological Modeling

In the HOBE project, integrated hydrological modeling at catchment scale has been performed using MIKE SHE as the modeling platform. The model has been used for analyzing the impact of different bias correction methods for precipitation and for testing various data assimilation techniques and approaches.

The MIKE SHE model is capable of simulating traditional hydrological fluxes, such as stream flow, recharge, and groundwater inflow to streams as well as traditional state variables, such as stream water levels, soil moisture, and hydraulic heads. When the model is expanded with a soil–vegetation–atmosphere–transfer model (MIKE SHE SW-ET), the integrated modeling platform can provide simulations of additional fluxes in the form of sensible, latent, and ground heat fluxes as well as net radiation. Additional state variables can be simulated, such as land surface, soil, and canopy temperatures. Using the expanded model, it is possible to use the eddy covariance measurements from the flux stations as well as remotely sensed land surface temperature for calibration, validation, or assimilation in addition to traditional data in the form of stream flow, groundwater inflow, hydraulic head, and soil moisture.

The wealth of data generated by the HOBE observatory has been used for constraining integrated hydrological modeling. Different data types have different levels of importance in this regard. Stisen et al. (2018) used five independent types of spatio-temporal observations (stream discharge, groundwater head, latent heat flux, soil moisture, and remotely sensed land surface temperature) to formulate 11 objective functions focusing on bias and root mean square error (RMSE) of time series from multiple observation stations. A sensitivity analysis of 35 parameters showed that groundwater hydraulic parameters were the most sensitive, which was not surprising because the catchment is groundwater dominated. However, near-surface fluxes and states like soil moisture, evapotranspiration, and land surface temperature were also sensitive to groundwater parameters, illustrating the importance of including various types of data when calibrating an integrated hydrological model. The study documented that traditional data in the form of discharge and hydraulic head are required when

calibrating an integrated and distributed model; however, the model calibration is more robust when additional data are included.

Traditionally, hydrological models have been validated against aggregated performance metrics, such as discharge using, for example, the Nash–Sutcliffe coefficient. As hydrological models become more advanced and provide integrated and distributed descriptions of the catchment dynamics, there is an increasing awareness that such models need to be validated in a spatial context. Spatial model evaluation is particularly important using multiobjective calibration of distributed models. Koch et al. (2015) tested empirical orthogonal functions (EOF) and Kappa statistics (and extended by Fuzziness) as spatial evaluation metrics for validating distributed hydrological modeling results. The test on the Ahlergaarde catchment showed that the EOF analysis pinpointed a model deficiency with respect to the simulation of the groundwater table and that the Kappa statistics extended by Fuzziness was suitable for map comparison.

Climate Change and Hydrology

Climate change and the impact on hydrology have been subject to much research within the framework of HOBE. van Roosmalen et al. (2009) quantified the effects of climate change and land use change on water resources using the MIKE SHE model. The study showed that projected climate change was the dominating factor for the future hydrological conditions in the Skjern catchment. Other factors, such as land use changes and irrigation requirements, had much less hydrological impact.

Karlsson et al. (2014) analyzed the historical trends in hydrological variables for the Ahlergaarde catchment and showed that, during the last 133 yr, precipitation has increased by 26%, temperature by 1.4°C, discharge by 52%, and groundwater recharge by 86%. These results showed that the climatic conditions are highly nonstationary and that the observed trends started before the trend of the CO_2 concentration in the atmosphere changed. Moreover, the historical development in precipitation is larger than projected by most climatic models toward year 2100 (Seaby, 2013).

Lucatero et al. (2018) analyzed the skill and reliability of using raw and preprocessed seasonal ensemble meteorological forecasts from the European Center for Medium-Range Weather Forecasts as input into the MIKE SHE model for the Ahlergaarde catchment for generating streamflow predictions with lead times up to 7 mo. Ensemble meteorological forecasts are subject to bias, and the hydrological model is subject to structural bias. This leads to results where the error in the streamflow forecasts may be either compensated or inflated. The analysis showed that some prediction skill was seen for a lead time of 1 mo for the wettest months, which was due in part to compensational errors. Overall, streamflow forecasts based on climate model results did not show more skill than when based on ensemble historical meteorology.

Simulations by climate models at temporal and spatial scales relevant for assessments of hydrological impacts of climate change are subject to considerable uncertainties. Often the simulations by regional-scale climate models (RCMs) exhibit substantial biases that affect the credibility of future projections. In consequence, the reliability of the hydrological projections is also affected if the climate model projections serve as input into a hydrological model. In many climate models, the hydrological feedback from the land surface to the atmosphere and the subsurface flow are insufficiently described. One option to improve the reliability of climate model simulations is to include a dynamic coupling allowing for two-way exchanges of fluxes and variables between the climate model and the hydrological model, where the latter represent the surface and subsurface processes. Larsen et al. (2014, 2016b) report results based on a coupling between the HIRHAM RCM (Christensen et al., 2006) and the MIKE SHE hydrological model (Abbott et al., 1986) with the SWET land-surface scheme (Overgaard, 2005) included. In this coupling, HIRHAM provides the following climatic variables to MIKE SHE: precipitation, surface temperature, surface pressure, relative humidity, global radiation, and wind speed. The MIKE SHE model returns sensible heat and latent heat to HIRHAM. The results showed that the dynamic coupling particularly improved the simulation of precipitation by the RCM, including both extreme and convective precipitation events. This suggests that more realistic descriptions of both surface and subsurface processes are important for the simulation of climatic conditions. This is particularly true for the conditions in the Skjern catchment, where groundwater flow imposes high control on soil moisture and thus surface temperature and latent heat flux. The results suggest that the need for bias correction of simulations by dynamically coupled climate–hydrology models may be significantly reduced.

Coupled climate–hydrology models may provide an avenue for reducing the uncertainty of climate and hydrological projections. However, different climate models provide different results due to differences in model formulations and internal variability. Also, hydrological models are different in structure and parameterization and thus provide different predictions of climate change even though they have been calibrated to the same level of accuracy based on historical data (Karlsson et al., 2016).

Conclusions and Future Perspectives

During the lifetime of the HOBE observatory, a wealth of new observational data has been produced in the Skjern catchment on state variables, water fluxes, and parameters at different temporal and spatial scales. The observational data have been collected using traditional measurement techniques as well as innovative ground-based, airborne, and satellite-borne sensor techniques. Together with the historical monitoring data (e.g., for precipitation), which date back to 1870, the database has provided a platform for detailed analyses of the dynamics of individual hydrological processes, the interaction between hydrological compartments, and catchment and subcatchment scale responses using, among others, integrated hydrological modeling. Several interdisciplinary studies have been performed, and the observatory has formed the basis for testing and benchmarking of instrumentation, hypotheses, and

models. As an important outcome of the research, the hydrological fluxes are now determined with much more certainty, and the associated uncertainties are quantified (see, e.g., Sebok et al. [2016] and Ehlers [2018]). In line with this, the water balance is now better constrained at different spatial scales.

Almost 10 yr of continuous time series have been collected. This enables detailed insight into the seasonal and interannual dynamics and to some extent extreme climatic and hydrological events. Moreover, the time series is steadily approaching a length that also supports analyses of longer-term dynamics.

Building and maintaining an interdisciplinary hydrological observatory is a challenge because a variety of different instrumentation needs to be installed and maintained. The instrumentation collects data at different temporal and spatial scales, and these data need to be processed in different ways. It has been a continuing challenge to ensure that the instrumentation works properly and that the collected data are of acceptable quality and to make the data available to the project group in a timely manner. To be successful in this regard requires a dedicated and committed technical staff. The different hydrological compartments interact through the hydrological cycle, and thus scientists dedicated to research in a specific hydrological component are dependent on results from other components. Managing a hydrological observatory thus requires that the scientists involved are committed to interdisciplinary research and willing to share knowledge and data in a timely manner.

The HOBE observatory represents hydrological conditions in a temperate climate with relatively high precipitation and an associated high recharge due to the dominance of high-permeable sediments in the catchment. The stream discharge is therefore also groundwater dominated. The catchment is as such complementary to other hydrological observatories described in this special issue, and an infrastructure is provided for research of such hydrological regime.

The lifetime of HOBE is unsure. However, if the observatory continues, there are a number of research goals we would like to pursue, including (i) further development of weather radar-based quantitative regional precipitation estimation, (ii) regional estimation of ET and soil moisture from emerging satellite data, (iii) further development of the cosmic ray rover technique for establishing ground truth data on soil moisture at an appropriate temporal and spatial scale, (iv) further development of distributed temperature sensing along stream reaches to obtain data for regional scale surface water–groundwater interaction, (v) further development of airborne geophysical techniques for mapping of the geological architecture, (vi) further development of parameterization and calibration frameworks for improving the spatial patterns of distributed model simulations, and (vii) further development of techniques for uncertainty propagation in integrated hydrological modeling.

Acknowledgments

The VILLUM Foundation provided funding that made the HOBE observatory possible.

References

Abbott, M.B., J.C. Bathurst, J.A. Cunge, P.E. O'Connel, and J. Rasmussen. 1986. An introduction to the European hydrological system–System Hydrologique European, SHE: 2. Structure of a physically-based, distributed modeling system. J. Hydrol. 87:61–77. doi:10.1016/0022-1694(86)90115-0

Allerup, P., and H. Madsen. 1980. Accuracy of point measurements. Nord. Hydrol. 11:57–70. doi:10.2166/nh.1980.0005

Allerup, P., H. Madsen, and F. Vejen. 1997. A comprehensive model for correcting point precipitation. Nord. Hydrol. 28:1–20. doi:10.2166/nh.1997.0001

Allerup, P., H. Madsen, and F. Vejen. 1998. Standard values for precipitation correction (1961–90). Tech. Rep. 98-10. Danish Meteorol. Inst., Copenhagen.

Andreasen, M., L.A. Andreasen, K.H. Jensen, T.O. Sonnenborg, and S. Bircher. 2013. Estimation of regional groundwater recharge using data from a distributed soil moisture network. Vadose Zone J. 12(3). doi:10.2136/vzj2013.01.0035

Andreasen, M., K.H. Jensen, D. Desilets, T.F. Franz, M. Zreda, H.R. Bogena, and M.C. Looms. 2017a. Status and perspectives of the cosmic-ray neutron method for soil moisture estimation and other environmental science applications. Vadose Zone J. 16(8). doi:10.2136/vzj2017.04.0086

Andreasen, M., K.H. Jensen, D. Desilets, M. Zreda, H. Bogena, and M.C. Looms. 2017b. Cosmic-ray neutron transport at a forest field site: Sensitivity analysis to different environmental conditions with focus on biomass and canopy interception. Hydrol. Earth Syst. Sci. 21:1875–1894. doi:10.5194/hess-21-1875-2017

Andreasen, M., K.H. Jensen, M. Zreda, D. Desilets, H. Bogena, and M.C. Looms. 2016. Modeling cosmic-ray neutron field measurements. Water Resour. Res. 52:6451–6471. doi:10.1002/2015WR018236

Auken, E., A.V. Christiansen, C. Kirkegaard, G. Fiandaca, C. Schamper, A.A. Behroozmand, et al. 2014. An overview of a highly versatile forward and stable inverse algorithm for airborne, ground-based and borehole electromagnetic and electric data. Explor. Geophys. 46:223–235. doi:10.1071/EG13097

Binley, A., S.S. Hubbard, J.A. Huisman, A. Revil, D.A. Robinson, K. Singha, and L.D. Slater. 2015. The emergence of hydrogeophysics for improved understanding of subsurface processes over multiple scales. Water Resour. Res. 51:3837–3866. doi:10.1002/2015WR017016

Bircher, S., J.E. Balling, N. Skou, and Y. Kerr. 2012a. Validation of SMOS brightness temperatures during the HOBE airborne campaign, western Denmark. IEEE Trans. Geosci. Remote Sens. 50:1468–1482. doi:10.1109/TGRS.2011.2170177

Bircher, S., N. Skou, K.H. Jensen, J.P. Walker, and L. Rasmussen. 2012b. A soil moisture and temperature network for SMOS validation in western Denmark. Hydrol. Earth Syst. Sci. 16:1445–1463. doi:10.5194/hess-16-1445-2012

Bircher, S., N. Skou, and Y. Kerr. 2013. Validation of SMOS L1C and L2 products and important parameters of the retrieval algorithm in the Skjern River catchment, western Denmark. IEEE Trans. Geosci. Remote Sens. 51:2969–2985. doi:10.1109/TGRS.2012.2215041

Christensen, O.B., M. Drews, J.H. Christensen, K. Dethloff, K. Ketelsen, I. Hebestadt, and A. Rinke. 2006. The HIRHAM regional climate model version 5. Rep. 06-17. Danish Meteorol. Inst., Copenhagen.

Colliander, A., T.J. Jackson, S.K. Chana, P. O'Neill, R. Bindlish, M.H. Cosh, et al. 2018. An assessment of the differences between spatial resolution and grid size for the SMAP enhanced soil moisture product over homogeneous sites. Remote Sens. Environ. 207:65–70. doi:10.1016/j.rse.2018.02.006

Duque, C., S. Müller, E. Sebok, K. Haider, and P. Engesgaard. 2016. Estimating groundwater discharge to surface waters using heat as a tracer in low flux environments: The role of thermal conductivity. Hydrol. Processes 30:383–395. doi:10.1002/hyp.10568

Ehlers, L. 2018. Uncertainties in groundwater–surface water modelling for the HOBE catchment. Ph.D. diss. Univ. of Copenhagen, Denmark.

Frederiksen, R.R. 2017. Surface–groundwater interaction: Elements of the hydrograph on a hill island. Ph.D. diss. Aarhus Univ., Denmark.

Fu, S., T. Sonnenborg, K.H. Jensen, and X. He. 2011. Impact of precipitation spatial resolution on the hydrological response of an integrated distributed water resources model. Vadose Zone J. 10:25–36. doi:10.2136/vzj2009.0186

Goodison, B.E., P.Y.T. Louie, and D. Yang. 1998. WMO solid precipitation measurement intercomparison. Rep. 67. World Meteorol. Organiz., Geneva, Switzerland.

Greve, M.H., M.B. Greve, P.K. Bocher, T. Balstrom, H. Breuning-Madsen, and L. Krogh. 2007. Generating a Danish raster-based topsoil property map combining choropleth maps and point information. Dan. J. Geogr. 107(2):1–12. doi:10.1080/00167223.2007.10649565

Guzinski, R., M.C. Anderson, W.P. Kustas, H. Nieto, and I. Sandholt. 2013. Using a thermal-based two source energy balance model with time-differencing to estimate surface energy fluxes with day-night MODIS observations. Hydrol. Earth Syst. Sci. 17:2809–2825. doi:10.5194/hess-17-2809-2013

Guzinski, R., H. Nieto, R. Jensen, and G. Mendiguren. 2014. Remotely sensed land-surface energy fluxes at sub-field scale in heterogeneous agricultural landscape and coniferous plantation. Biogeosciences 11:5021–5046. doi:10.5194/bg-11-5021-2014

Guzinski, R., H. Nieto, S. Stisen, and R. Fensholt. 2015. Inter-comparison of energy balance and hydrological models for land surface energy fluxes estimation over a whole river catchment. Hydrol. Earth Syst. Sci. 19:2017–2036. doi:10.5194/hess-19-2017-2015

Haarder, E.B. 2014. Hydrogeophysical investigations of unsaturated flow and transport. Ph.D. diss. Dep. Geosci. Nat. Resour. Manage., Univ. of Copenhagen, Denmark.

Haarder, E.B., A. Binley, M.C. Looms, J. Doetsch, L. Nielsen, and K.H. Jensen. 2012. Comparing plume characteristics inferred from cross-borehole geophysical data. Vadose Zone J. 11(4). doi:10.2136/vzj2012.0031

Haarder, E.B., K.H. Jensen, A. Binley, L. Nielsen, T.B. Uglebjerg, and M.C. Looms. 2015. Estimation of recharge from long-term monitoring of saline tracer transport using electrical resistivity tomography. Vadose Zone J. 14(7). doi:10.2136/vzj2014.08.0110

Haider, K., P. Engesgaard, T.O. Sonnenborg, and C. Kirkegaard. 2015. Numerical modeling of salinity distribution and submarine groundwater discharge to a coastal lagoon based on airborne electromagnetic data. Hydrogeol. J. 23:217–233. doi:10.1007/s10040-014-1195-0

Hansen, S. 2002. Daisy, a flexible soil–plant–atmosphere system model. Royal Veterinary and Agricultural Univ., Copenhagen, Denmark.

He, X., A.L. Højberg, F. Jørgensen, and J.C. Refsgaard. 2015. Assessing hydrological model predictive uncertainty using stochastically generated geological models. Hydrol. Processes 29:4293–4311. doi:10.1002/hyp.10488

He, X., K.H. Jensen, T.O. Sonnenborg, F. Jørgensen, A.-S. Høyer, and R.R. Møller. 2013a. Analyzing the effects of geological and parameter uncertainty on groundwater head and travel time. Hydrol. Earth Syst. Sci. 17:3245–3260. doi:10.5194/hess-17-3245-2013

He, X., J. Koch, C. Zheng, T. Bøvit, and K.H. Jensen. 2018. Comparison of simulated spatial patterns using rain gauge and polarimetric radar based precipitation data in catchment hydrological modeling. J. Hydrometeorol. 19:1273–1288. doi:10.1175/JHM-D-17-0235.1

He, X., T. Sonnenborg, F. Jørgensen, and K.H. Jensen. 2014. The effect of training image and secondary data integration with multiple-point geostatistics in groundwater modeling. Hydrol. Earth Syst. Sci. 18:2943–2954. doi:10.5194/hess-18-2943-2014

He, X., T.O. Sonnenborg, F. Jørgensen, and K.H. Jensen. 2017. Modelling a real-world buried valley system with vertical non-stationarity using multiple-point statistics. Hydrogeol. J. 25:359–370. doi:10.1007/s10040-016-1486-8

He, X., T.O. Sonnenborg, J.C. Refsgaard, F. Vejen, and K.H. Jensen. 2013b. Evaluation of the value of radar QPE data and rain gauge data for hydrological modeling. Water Resour. Res. 49:5989–6005. doi:10.1002/wrcr.20471

He, X., F. Vejen, S. Stisen, T. Sonnenborg, and K.H. Jensen. 2011. An operational weather radar–based quantitative precipitation estimation and its application in catchment water resources modeling. Vadose Zone J. 10:8–24. doi:10.2136/vzj2010.0034

Henriksen, H.J., L. Troldborg, P. Nyegaard, T.O. Sonnenborg, J.C. Refsgaard, and B. Madsen. 2003. Methodology for construction, calibration and validation of a national hydrological model for Denmark. J. Hydrol. 280:52–71. doi:10.1016/S0022-1694(03)00186-0

Herbst, M., T. Friborg, R. Ringgaard, and H. Soegaard. 2011. Catchment-wide atmospheric greenhouse gas exchange as influenced by land use diversity. Vadose Zone J. 10:67–77. doi:10.2136/vzj2010.0058

Hoffmann, H., R. Jensen, A. Thomsen, H. Nieto, J. Rasmussen, and T. Friborg. 2016a. Crop water stress maps for an entire growing season from visible and thermal UAV imagery. Biogeosciences 13:6545–6563. doi:10.5194/bg-13-6545-2016

Hoffmann, H., H. Nieto, R. Jensen, R. Guzinski, P. Zarco-Tejada, and T. Friborg. 2016b. Estimating evaporation with thermal UAV data and two-source energy balance models. Hydrol. Earth Syst. Sci. 20:697–713. doi:10.5194/hess-20-697-2016

Houmark-Nielsen, M., and K.H. Kjaer. 2003. Southwest Scandinavia, 50-15 kyr BP: Palaeogeography and environmental change. J. Quat. Sci. 18:769–786. doi:10.1002/jqs.802

Jensen, J.K., and P. Engesgaard. 2011. Nonuniform groundwater discharge across a streambed: Heat as a tracer. Vadose Zone J. 10:98–109. doi:10.2136/vzj2010.0005

Jensen, K.H., and T.H. Illangasekare. 2011. HOBE: A hydrological observatory in Denmark. Vadose Zone J. 10:1–7. doi:10.2136/vzj2011.0006

Jougnot, D., N. Linde, E.B. Haarder, and M.C. Looms. 2015. Monitoring of saline tracer movement with vertically distributed self-potential measurements at the HOBE agricultural test site, Voulund, Denmark. J. Hydrol. 521:314–327. doi:10.1016/j.jhydrol.2014.11.041

Karan, S., P. Engesgaard, M.C. Looms, T. Laier, and J. Kazmierczak. 2013. Groundwater flow and mixing in a wetland-stream system: Field study and numerical modeling. J. Hydrol. 488:73–83. doi:10.1016/j.jhydrol.2013.02.030

Karan, S., P. Engesgaard, and J. Rasmussen. 2014. Dynamic streambed fluxes during rainfall–runoff events. Water Resour. Res. 50:2293–2311. doi:10.1002/2013WR014155

Karan, S., E. Sebok, and P. Engesgaard. 2017. Air/water/sediment temperature contrasts in small streams to identify groundwater seepage locations. Hydrol. Processes 31:1258–1270. doi:10.1002/hyp.11094

Karlsson, I.B., T. Sonnenborg, K.H. Jensen, and J.C. Refsgaard. 2014. Historical trends in precipitation and stream discharge at the Skjern River catchment, Denmark. Hydrol. Earth Syst. Sci. 18:595–610. doi:10.5194/hess-18-595-2014

Karlsson, I.B., T.O. Sonnenborg, J.C. Refsgaard, D. Trolle, C.D. Borgesen, J.E. Olesen, et al. 2016. Combined effects of climate models, hydrological model structures and land use scenarios on hydrological impacts of climate change. J. Hydrol. 535:301–317. doi:10.1016/j.jhydrol.2016.01.069

Kerr, Y., P. Waldteufel, J.-P. Wigneron, J.-M. Martinuzzi, J. Font, and M. Berger. 2001. Soil moisture retrieval from space: The Soil Moisture and Ocean Salinity (SMOS) mission. IEEE Trans. Geosci. Remote Sens. 39:1729–1735. doi:10.1109/36.942551

Kirkegaard, C., T. Sonnenborg, E. Auken, and F. Jørgensen. 2011. Salinity distribution in heterogeneous coastal aquifers mapped by airborne electromagnetics. Vadose Zone J. 10:125–135. doi:10.2136/vzj2010.0038

Koch, J., X. He, K.H. Jensen, and J.C. Refsgaard. 2014. Challenges in conditioning a stochastic geological model of a heterogeneous glacial aquifer to a comprehensive soft data set. Hydrol. Earth Syst. Sci. 18:2907–2923. doi:10.5194/hess-18-2907-2014

Koch, J., K.H. Jensen, and S. Stisen. 2015. Towards a true spatial model evaluation in distributed hydrological modeling: Kappa statistics, fuzzy theory and EOF-analysis benchmarked by the human perception and evaluated against a modeling case study. Water Resour. Res. 51:1225–1246. doi:10.1002/2014WR016607

Larsen, M.A.D., J.H. Christensen, M. Drews, M.B. Butts, and J.C. Refsgard. 2016b. Local control on precipitation in a fully coupled climate–hydrology model. Sci. Rep. 6:22927. doi:10.1038/srep22927

Larsen, M.A.D., J.C. Refsgaard, M. Drews, M.J.C. Butts, K.H. Jensen, J.H. Christensen, and O.B. Christensen. 2014. Results from a full coupling of the HIRHAM regional climate model and the MIKE SHE hydrological model for a Danish catchment. Hydrol. Earth Syst. Sci. 18:4733–4749. doi:10.5194/hess-18-4733-2014

Larsen, M.A.D., J.C. Refsgaard, K.H. Jensen, M.B. Butts, S. Stisen, and M. Mollerup. 2016a. Calibration of a distributed hydrology and land surface model using energy flux measurements. Agric. For. Meteorol. 217:74–88. doi:10.1016/j.agrformet.2015.11.012

Lucatero, D., H. Madsen, J.C. Refsgaard, J. Kidmose, and K.H. Jensen. 2018. Seasonal streamflow forecasts in the Ahlergaarde catchment, Denmark: Effect of preprocessing and postprocessing on skill and reliability. Hydrol. Earth Syst. Sci. 22:3601–3617. doi:10.5194/hess-22-3601-2018

Moffat, A.M., D. Papale, M. Reichstein, V. Hollinger, V. Richardson, A.G. Barr, et al. 2007. Comprehensive comparison of gap-filling techniques for eddy covariance net carbon fluxes. Agric. For. Meteorol. 147:209–232. doi:10.1016/j.agrformet.2007.08.011

Müller, S. 2016. Stable oxygen-18 and deuterium isotopes. Ph.D. diss. Dep. Geosci. Nat. Resour. Manage., Univ. of Copenhagen, Denmark.

Müller, S., C. Stumpp, J.H. Sørensen, N.W. Nielsen, and S. Jessen. 2017. Spatiotemporal variation of stable isotopic composition in precipitation: Post-condensational effects in a humid area. Hydrol. Processes 31:3146–3159. doi:10.1002/hyp.11186

Norman, J.M., W.P. Kustas, and K.S. Humes. 1995. Source approach for estimating soil and vegetation energy fluxes in observations of directional radiometric surface temperature. Agric. For. Meteorol. 77:263–293. doi:10.1016/0168-1923(95)02265-Y

Norman, J.M., W.P. Kustas, J. Prueger, and G. Diak. 2000. Surface flux estimation using radiometric temperature: A dual-temperature-difference method to minimize measurement errors. Water Resour. Res. 36:2263–2274. doi:10.1029/2000WR900033

Overgaard, J. 2005. Energy-based land-surface modelling: New opportunities in integrated hydrological modeling. Ph.D. diss. Inst. Environ. Resour., Technical Univ. of Denmark, Lyngby.

Poulsen, J.R., E. Sebok, D. Tetzlaff, and P. Engesgaard. 2015. Detecting groundwater discharge dynamics from point-to-catchment scale in a lowland stream: Combining hydraulic and tracer methods. Hydrol. Earth Syst. Sci. 19:1871–1886. doi:10.5194/hess-19-1871-2015

Rasmussen, J., H. Madsen, K.H. Jensen, and J.C. Refsgaard. 2015. Data assimilation in integrated hydrological modeling using ensemble Kalman filtering: Evaluating the effect of ensemble size and localization on filter performance. Hydrol. Earth Syst. Sci. 19:2999–3013. doi:10.5194/hess-19-2999-2015

Rasmussen, J., H. Madsen, K.H. Jensen, and J.C. Refsgaard. 2016. Data assimilation in integrated hydrological modelling in the presence of observation bias. Hydrol. Earth Syst. Sci. 20:2103–2118. doi:10.5194/hess-20-2103-2016

Reichle, R.H., G.J. De Lannoy, Q. Liu, J.V. Ardizzone, A. Colliander, A. Conaty, et al. 2017. Assessment of the SMAP Level-4 surface and root-zone soil moisture product using in situ measurements. J. Hydrometeorol. 18:2621–2645. doi:10.1175/JHM-D-17-0063.1

Ridler, M.E., H. Madsen, S. Stisen, S. Bircher, and R. Fensholt. 2014. Assimilation of SMOS derived soil moisture in a soil–vegetation–atmosphere transfer model in western Denmark. Water Resour. Res. 50:8962–8981. doi:10.1002/2014WR015392

Ridler, M.E., D. Zhang, H. Madsen, J. Kidmose, J.C. Refsgaard, and K.H. Jensen. 2017. Bias-aware data assimilation in integrated hydrological modelling. Hydrol. Res. 49:989–1004. doi:10.2166/nh.2017.117

Ringgaard, R., H. Herbst, and T. Friborg. 2012. Partitioning of forest evapotranspiration: The impact of edge effects and canopy structure. Agric. For. Meteorol. 166–167:86–97. doi:10.1016/j.agrformet.2012.07.001

Ringgaard, R., H. Herbst, and T. Friborg. 2014. Partitioning forest evapotranspiration: Interception evaporation and the impact of canopy structure, local and regional advection. J. Hydrol. 517:677–690. doi:10.1016/j.jhydrol.2014.06.007

Ringgaard, R., M. Herbst, T. Friborg, K. Schelde, A.G. Thomsen, and H. Søgaard. 2011. Energy fluxes above three disparate surfaces in a temperate mesoscale coastal catchment. Vadose Zone J. 10:54–66. doi:10.2136/vzj2009.0181

Scharling, M., K. Rajakumar, L. Hansen, and J.J. Jensen. 2006. Catalogue of meteorological observing stations operated by DMI. DMI Internal Rep. Danish Meteorol. Inst., Copenhagen.

Scharling, P., E.S. Rasmussen, T.O. Sonnenborg, P. Engesgaard, and K. Hinsby. 2009. Three-dimensional regional-scale hydrostratigraphic modeling based on sequence stratigraphic methods: A case study of the Miocene succession in Denmark. Hydrogeol. J. 17:1913–1933. doi:10.1007/s10040-009-0475-6

Schelde, K., R. Ringgaard, M. Herbst, A. Thomsen, T. Friborg, and H. Søgaard. 2011. Comparing evapotranspiration rates estimated from atmospheric flux and TDR soil moisture measurements. Vadose Zone J. 10:78–83. doi:10.2136/vzj2010.0060

Seaby, L.P. 2013. Uncertainty in hydrological change modelling. Ph.D. diss. Dep. Geosci. Nat. Resour. Manage., Univ. of Copenhagen, Denmark.

Sebok, E., C. Duque, P. Engesgaard, and E. Bøgh. 2015. Application of distributed temperature sensing for coupled mapping of sedimentation processes and spatio-temporal variability of groundwater discharge in soft-bedded streams. Hydrol. Processes 29:3408–3422. doi:10.1002/hyp.10455

Sebok, E., C. Duque, J. Kazmierczak, P. Engesgaard, B. Nilsson, S. Karan, and M. Frandsen. 2013. High-resolution distributed temperature sensing to detect seasonal groundwater discharge into Lake Væng, Denmark. Water Resour. Res. 49:5355–5368. doi:10.1002/wrcr.20436

Sebok, E., J.C. Refsgaard, J.J. Warmink, S. Stisen, and K.H. Jensen. 2016. Using expert elicitation to quantify the water balance and its uncertainties for two nested catchments. Water Resour. Res. 52:5111–5131. doi:10.1002/2015WR018461

Selker, J.S., L. Thevenaz, H. Huwald, A. Mallet, W. Luxemburg, N. van de Giesen, et al. 2006. Distributed fiber-optic temperature sensing for hydrologic systems. Water Resour. Res. 42:W12202. doi:10.1029/2006WR005326

Stisen, S., A.L. Højbjerg, J.C. Refsgaard, T. Sonnenborg, and L. Troldborg. 2011. Evaluation of climate input biases and water balance issues using a coupled surface-subsurface model. Vadose Zone J. 10:37–53. doi:10.2136/vzj2010.0001

Stisen, S., A.L. Højberg, L. Troldborg, J.C. Refsgaard, B.S.B. Christensen, M. Olsen, and H.J. Henriksen. 2012. On the importance of appropriate precipitation gauge catch correction for hydrological modelling at mid to high latitudes. Hydrol. Earth Syst. Sci. 16:4157–4176. doi:10.5194/hess-16-4157-2012

Stisen, S., J. Koch, T.O. Sonnenborg, J.C. Refsgard, S. Bircher, R. Ringgaard, and K.H. Jensen, 2018. Moving beyond runoff calibration: Multi-variable optimization of a surface–subsurface–atmosphere model. Hydrol. Processes 32:2654–2668. doi:10.1002/hyp.13177

Sørensen, K., and E. Auken. 2004. SkyTEM: A new high-resolution helicopter transient electromagnetic system. Explor. Geophys. 35:194–202. doi:10.1071/EG04194

van Roosmalen, L., B.S.B. Christensen, and T.O. Sonnenborg. 2007. Regional differences in climate change impacts on groundwater and stream discharge in Denmark. Vadose Zone J. 6:554–571. doi:10.2136/vzj2006.0093

van Roosmalen, L., T.O. Sonnenborg, and K.H. Jensen. 2009. Quantifying the effects of climate change and land use change on water resources in Denmark using an integrated watershed model. Water Resour. Res. 45:W00A15. doi:10.1029/2007WR006760

Vasquez, V. 2013. Profile soil water content measurements for estimation of groundwater recharge in different land uses. Ph.D. diss. Science and Technology, Aarhus Univ., Denmark.

Vásquez, V., A. Thomsen, B. Iversen, K. Schelde, and R. Ringgaard. 2015. Integrating lysimeter drainage and eddy covariance flux measurements in a groundwater recharge model. J. Hydrol. Sci. 60:1520–1537. doi:10.1080/02626667.2014.904964

Vereecken, H., J.A. Huisman, H.J. Hendricks Franssen, N. Brüggemann, H.R. Bogena, S. Kollet, et al. 2015. Soil hydrology: Recent methodological advances, challenges, and perspectives. Water Resour. Res. 51:2616–2633. doi:.10.1002/2014WR016852

Zhang, D., H. Madsen, M.E. Ridler, J. Kidmose, K.H. Jensen, and J.C. Refsgaard. 2016. Multivariate hydrological data assimilation of soil moisture and groundwater head. Hydrol. Earth Syst. Sci. 20:4341–4357. doi:10.5194/hess-20-4341-2016

Zhang, D., H. Madsen, M.E. Ridler, J.C. Refsgaard, and K.H. Jensen. 2015. Impact of uncertainty description on assimilating hydraulic head in the MIKE SHE distributed hydrological model. Adv. Water Resour. 86:400–413. doi:10.1016/j.advwatres.2015.07.018.